THE ASTRONOMICAL JOURNAL

FOUNDED BY B. A. GOULD

PUBLISHED BY THE AMERICAN ASTRONOMICAL SOCIETY

VOLUME 64 1959 May ~ No. 1269 *NUMBER 4*

ONE HUNDRED–SECOND MEETING OF THE AMERICAN ASTRONOMICAL SOCIETY, ROCHESTER, NEW YORK, MARCH 30–APRIL 2, 1959

ABSTRACTS OF PAPERS PRESENTED

ABELL, GEORGE O. **The luminosity function of the Coma cluster of galaxies.**

A program is in progress to determine the bright end of the luminosity function of each of about 30 rich clusters of galaxies with a technique of extrafocal photographic photometry with the 48-inch Schmidt telescope of the Palomar Observatory.

Magnitudes of a number of stars in each cluster field are calibrated by photographic and/or photoelectric methods. Then magnitudes of galaxies are obtained by comparing images of galaxies with the calibrated stars on each of five plates taken at various amounts out of focus. The measures are made in two colors corresponding, approximately, to international photographic and photovisual magnitudes.

The integrated magnitude for each galaxy is obtained from the surface brightness of its images on two or more extrafocal plates through a method developed by Abell and Mihalas which utilizes a knowledge of the ellipticity and an assumed distribution of surface brightness of the galaxy.

The luminosity function has been determined completely for the first of the clusters, the Coma cluster of galaxies. Near the limit of the observations, $m_{pg} = 19.2$, the luminosity function increases rapidly. However, about two magnitudes below the bright end of the luminosity function there is a marked preliminary maximum. It is necessary to count through about the first 150 brightest galaxies to reach this maximum. About three magnitudes fainter than the brightest cluster members there is a minimum; at still fainter magnitudes the luminosity function increases rapidly. The preliminary maximum exists in the luminosity functions of galaxies of both small (<0.4) and large color indices.

If further investigation shows that this maximum near the bright end is common to the luminosity functions of galaxies in the other rich clusters, it should provide a new, more reliable distance criterion for rich clusters of galaxies.

Department of Astronomy,
University of California,
Los Angeles, Calif.

CAMERON, A. G. W. **Carbon thermonuclear reactions and heavy-element formation.**

When helium is consumed at a high rate of energy generation in massive stars and in shell sources of somewhat less massive stars, the principal product is C^{12}. Following helium exhaustion, carbon thermonuclear reactions provide the next source of energy generation. In these reactions both protons and alpha-particles are produced; a theoretical estimate gives comparable yields for these two types of particles. In the earlier stages of carbon-burning, the protons are captured by C^{12}, forming C^{13}, and the alpha-particles react with the C^{13} to produce neutrons. Cross sections were calculated from experimental data or by theoretical methods for a large number of reactions which could have any important effect on the abundances; these include (α, γ), (α, p), (α, n), (p, γ), (p, α), and (n, γ) reactions. Changes in abundances of a wide variety of nuclei taking place during carbon-burning were followed with the aid of a computer. The main products, formed with comparable abundances, are O^{16}, Ne^{20}, Na^{23} and Mg^{24}. If the gas was originally pure hydrogen, then heavy elements are formed by neutron capture on a slow time scale and build up to abundances comparable to heavy element abundances in the sun. In a Population I star containing ten per cent of the solar abundances in the neon to iron region, the heavy elements become overabundant with respect to solar composition by a factor of about 1000. In a star of solar composition the heavy elements become overabundant by a factor of 10,000. These large overabundance factors are reached in the very early stages of carbon-burning. This process is free from the difficulties associated with other suggested mechanisms of neutron production, but it is required that the ratio of proton to alpha-particle production in carbon-burning should not differ from the theoretical estimate by much more than an order of magnitude in either direction.

Atomic Energy of Canada Limited,
Chalk River, Ontario

CHAPMAN, SYDNEY AND ALLER, L. H. **Diffusion in the sun.**

The rate at which a heavy ionized atom will sink towards the interior of the sun will depend on the logarithmic pressure and temperature gradients. The coefficient of diffusion depends on the mass of the ion, its charge, and the Debye length. Thermal diffusion is much more important than other types. The rate of diffusion is greater in the outer layers of the sun but only the value at the bottom of the convection zone is important in altering the composition of the superficial layers. Calculations carried out for lead, iron, and silicon indicate that the Pb/Si and Fe/Si ratios may have been altered by appreciable amounts in the course of the last five thousand million years. An accurate value must await a better knowledge of the solar convection zone and an improved theory of diffusion. The presence of heavy metals in the sun's atmosphere with abundances roughly comparable with those in meteorites indicates that diffusion has probably not drastically altered the composition of the superficial layers and speaks in favor of a convection zone of the order of 0.2 of a solar radius.

University of Alaska,
College, Alaska
The University of Michigan,
Ann Arbor, Mich.

DONN, BERTRAM. **Comets and the chemistry of matter in space.**

Whipple's icy-conglomerate comet model serves as a starting point for studying space chemistry. From the observational data on comets one can deduce information about the primitive state of condensed material. By relating comets to recent work on low temperature chemistry further knowledge about the composition, structure, and origin of comets may be obtained. The combination of these approaches leads to a means of developing a consistent theory of cosmic chemistry at low temperatures.

There is considerable support for the picture of a large comet reservoir at large solar distances where temperatures are very low. Even close to the sun comets remain cold—about 150°K—because of the release of volatile gases. Because of small mass and radius no appreciable internal heating has taken place. Consequently no extensive chemical changes have occurred since their accumulation and comets still are representative of their initial state. Comets may be looked upon as the initial stages of accumulation from the solar nebula which, if continued, would have ultimately developed into asteroidal and planetary objects.

Meteors appear to be fragile, fluffy particles with essentially all having a cometary origin. The meteors released from the icy matrix must have been acquired with the same structure as we now observe them. They therefore indicate that solid particles can grow in space with the intricate structures characteristic of growth in the laboratory. This should also be true for interstellar particles composed of condensed molecules. These considerations have a bearing on rate of growth.

Recent experiments tend to rule out high concentrations of radicals in solids as originally proposed by Donn and Urey. Laboratory values run around 0.1 per cent instead of the 10 per cent suggested. However, similar work indicates that significant amounts of reactive molecules may be produced by incident radicals. Energy in form of excited molecules may also be stored. Thus, chemical energy to produce comet phenomena still would be available.

One must be careful not to deduce comet properties from terrestrial or meteoric results as the thermal history of comets and of the latter class of objects have been completely different. The behavior of sulfur in comets will be used as an example.

A wide variety of observational studies as well as experimental and theoretical programs are suggested by this approach to cosmic chemistry.

This investigation was supported by a National Science Foundation grant to Wayne State University and a Department of the Army contract with the Free Radical Section of the National Bureau of Standards.

Department of Physics,
Wayne State University,
Detroit, Mich.

FIREMAN, E. L. AND DEFELICE, J. **Argon-39 and tritium in meteorites.**

The radioactive isotopes A^{39} (260-year half-life) and tritium (12.4-year half-life) were measured in seven iron and in two stony meteorites. A^{39} was detected and measured in the iron meteorites Sikhote-Alin (1947), Treysa (1916), Pitts (1921), and in the stony meteorites Norton County (1948) and St. Michel (1910). The detection and measurement of A^{39} in these meteorites makes it possible to determine their argon exposure ages (Fireman, E. L. *Nature*, **181**, 1613, 1958). On the basis of the same assumptions used in that article, the ages are 4.9×10^8 years for the Sikhote-Alin meteorite, 5.7×10^8 years for the Treysa meteorite, 6.5×10^8 years for the Norton County meteorite, 1.7×10^8 years for the St. Michel meteorite, and, for the Pitts meteorite, an unusually low figure in the range of 10^7 years.

The short argon exposure ages may be interpreted in two ways: they may result from the loss of shielding material, worn off the meteorite in space by interplanetary dust and gas (suggested in private discussion with Professor Fred L. Whipple); or they may represent the times since the breakup of planets. From the lack of A^{39} in the Carbo and Grant meteorites and the small amount of A^{39} in the Washington County meteorite whose dates of fall are unknown, one can conclude that Carbo and Grant fell more than 1500 years ago and that the Washington County meteorite fell about 1000 years ago. In the case of the Cañon Diablo meteorite the He^3 content is so low that the measured absence of A^{39} and tritium does not necessarily mean that it fell long ago.

The ratio of tritium to A^{39} radioactivities (decays g^{-1} min^{-1}) in the Norton County meteorite is 230 to 1 at the time of fall. This ratio in the Sikhote-Alin meteorite is anomalously low being less than 1 to 1 at the time of fall.

The work was supported in part by a grant from the Atomic Energy Commission.

Smithsonian Astrophysical Observatory,
Cambridge, Mass.

GAPOSCHKIN, SERGEI. **On γ Velorum, ϵ Carinae and a Carinae as eclipsing variables.**

γ Velorum, a first-magnitude object, is the brightest star within a large region of the sky, so that no suitable comparison stars can be found on the usual plates of the Harvard collection. ζ Puppis, about .4 mag. fainter and eight degrees away, was used to estimate its brightness. Since both stars are excessively bright on the plates recently taken, I availed myself mostly of earlier plates taken prior to 1920. In addition, during my stay in Australia in the years 1956 and 1957, I estimated the star's brightness visually and obtained several dozen spectrograms for radial velocities. The data indicate that γ Velorum is very possibly an eclipsing variable with a small range, but the following parameters should be considered tentative because the scatter of observations in both brightness and velocity is equal to or even greater than the ranges themselves, especially in radial velocities.

Photometric

Period = $16^{\mathrm{d}}.2334$
Epoch = 2435905.025JD (observed)
$A_1 = 1^{\mathrm{m}}.65 - 1^{\mathrm{m}}.84$
$A_2 = 1.65 - 1.78$
$D_1 = D_2? = 0^{\mathrm{p}}.09$
$k = 0.39$
$i = 84^{\circ}.5$

Spectroscopic

$K_{O,1} = 142$ km/sec (absorption)
$K_{W,2} = 174$ km/sec (emission)
$(a_1 + a_2) \sin i = 70.4 \times 10^6$ km
$(m_1 + m_2) \sin^3 i = 53.2 \odot$

Absolute

$R_O = 0.123a = 12.5 \odot$
$R_W = 0.049a = 5.0 \odot$
$Mu_O = 29.71 \odot$
$Mu_W = 24.23 \odot$
$M_{\mathrm{vis}}(\mathrm{system}) = -6^{\mathrm{m}}.7$

While making estimations, I noticed that the bright yellow star ϵ Carinae, a Carinae, and very possibly ι Carinae undergo definite changes of brightness, amounting to about 0.3 mag. The period of ϵ Carinae is about 785 days and the photographic range 3.57–3.83 mag.; the period of a Carinae is 6.751154 days and the ranges are 3.20–3.56 and 3.20–3.52 mag. ι Carinae has a very strong color, making it very difficult to estimate the brightness of its close neighbor, a Carinae.

Harvard College Observatory,
Cambridge, Mass.

HELFER, H. L. **On the velocity field of the nearby interstellar hydrogen.**

This is a progress report upon the analysis of the 21-cm survey for $|b| \geq 20^\circ$, undertaken at the Department of Terrestrial Magnetism, Carnegie Institute of Washington, and reported upon previously (Erickson, Helfer and Tatel 1959). Rough agreement between Shain's local magnetic pole of the Galaxy (Shain 1957) and the crudely defined pole of the high-latitude interstellar hydrogen suggests that the distribution of the interstellar gas is quite dependent upon the local magnetic field and that the possibility that the velocity-distance relation for the gas is different from that of the stars cannot be ignored.

As reported previously, the high latitude 21-cm line profiles give evidence of significant large-scale structure. Accordingly, a solution for the velocity-distance relation of the nearby gas was attempted. Including only first order terms one may write for the radial velocity:

$$V(l, b) = a + sR,$$

where R is the distance and

$$s = K + \cos^2 b\,(C + B_1 \sin 2l + B_2 \cos 2l) + (A_1 \sin l + A_2 \cos l) \sin 2b,$$

$$a = W_1 \cos l \cos b + W_2 \sin l \cos b + W_3 \sin b.$$

Using subjective estimates of the peak or center of line-profile velocities, solutions for the relative ratios, $K : C : B_1 : B_2 : A_1 : A_2$, were determined from the seven available values of (l, b) for which $V(l, b) + V(l + 180^\circ, -b) = 0$. The preliminary values are: 1.000, −0.820, −0.311, −0.182, +0.743, −0.322, in the order given above. The figures quoted are probably already influenced slightly by the occurrence of second order terms, their influence being evident in the observations taken at $b = \pm 20^\circ$.

The values of W_1, W_2, W_3, determined from the value of $V(l, b) - V(l + 180^\circ, -b)$ at the aforementioned zero points, are found to be 1.24 km/sec, 2.62 km/sec, −1.60 km/sec, respectively, but these values are quite crude. If accepted literally, this would suggest that the circular velocity of the local gas is about 3 km/sec faster than that of the stars.

The coordinate system used is that defined by the Lund Tables (Ohlsson, Reiz and Torgård 1956) with galactic center at $l \sim 327^\circ$, $b \sim -1^\circ$, and the velocity scale origin is the local stellar standard of rest, as given by the Lund Tables (MacRae and Westerhout 1956). This work was supported in part by the U.S. Air Force under Contract No. AF49(638)-52.

REFERENCES

Erickson, W. C., Helfer, H. L. and Tatel, H. E. 1959, *URSI-IAU Radio Astron. Symp. Paris 1958*, in press.

MacRae, D. A. and Westerhout, G. 1956, *Tables for the Reduction of Velocities to the Local Standard of Rest*, Lund Observatory.

Ohlsson, J., Reiz, A. and Torgård, I. 1956, *Tables for the Conversion of Galactic into Equatorial Coordinates*, Lund Observatory.

Shain, G. A. 1957, *Russian A. J.* **34**, 3.

Department of Physics and Astronomy,
University of Rochester,
Rochester, N. Y.

HERBIG, G. H. **Observations and an interpretation of VV Puppis.**

VV Puppis was discovered by Van Gent in 1931 and for a time was the variable star of shortest known period, 100 minutes. It differed from other ultra-short-period RR Lyrae-like stars, however, in that the rise to maximum light was much slower than the subsequent decline. It was also found that the light curve of VV Puppis frequently varied in shape, and that there was a slow change in the mean brightness of the system.

The mean (or minimum) brightness faded slowly in the years following discovery until in 1948–49 the star was found at a minimum m_{pg} near 17.0. Observations by Thackeray, Wesselink, and Oosterhoff at that time showed that the variations would sometimes cease for a considerable interval; there was one period of 18 days—over 200 cycles—when no variation above minimum light was observed. The peculiarity was compounded by the fact that when the light variations of VV Puppis resumed after an inactive interval, the maxima would again occur on the linear ephemeris that had held since discovery.

This latter fact pointed to the possibility that VV Puppis might not be a case of pulsation but rather of orbital motion, despite the curious light curve which is quite unlike that of an ordinary eclipsing variable. Spectroscopic observations made with the Crossley reflector in late 1958 (the star was about 1 mag. brighter than in 1948–49) demonstrated that VV Puppis is certainly not an RR Lyrae star: there is a hot continuum running well into the ultraviolet and the spectrum is dominated by strong emission lines of H and He II. No absorption spectrum can be seen. The displacements of the emission lines vary through a large range in the 100-minute ycle, and can be represented by a set of single-ine spectroscopic elements with $K = 437$ km/ec and $e = 0.09$. The velocity variation proeeds in synchronization with the light cycle; pectroscopic conjunction, with the emission-ine star behind, occurs just after the steep lecline from maximum light.

It appears that the observational information iow available on VV Puppis can be explained in erms of the star being an eclipsing system of ather unusual properties, as well as the binary of shortest known period. The system is picured as composed of a dark component plus a arger, brighter star which has widespread surace activity responsible for the emission lines. The following side of the larger star also conains a bright, hot area which produces the trong continuous spectrum. The system is at naximum light when the "hot spot" is seen aproximately centrally on the disc, but when the econdary star moves across, the hot spot is uickly covered. But when the geometrical clipse is over, the hot area has vanished around he limb so that the system remains faint until he fringe of the hot area comes around the oposite limb. The brightness then rises slowly as nore and more of the hot area is exposed. This ccounts for the long "minimum" which lasts over ialf the cycle.

On this interpretation, the secular change in he brightness of the system is due to intrinsic ariation in the brightness of the larger star. The cycle-to-cycle changes in the light curve nust be largely due to variation in the size and rightness of the hot area.

One of the interesting features of the system of VV Puppis is that, contrary to what one night expect, the masses are not extremely mall. The spectroscopic mass function sets a ower limit on the mass of the fainter star, bout 0.6 ⊙. If the two components are of qual mass, both would have values of about .4 ⊙. The system is similar in many respects to UX Ursae Majoris, DQ Herculis, and RW Trianguli.

Lick Observatory,
University of California,
Mount Hamilton, Calif.

HUFFER, C. M. AND CODE, A. D. **A three-color study of the stream-of-gas star U Cephei.**

Among the first observations with the new 36-inch telescope of the Pine Bluff Station of the Washburn Observatory were photoelectric measures of the well-known eclipsing binary star U Cephei. On September 9, 1958, the first observations of the primary eclipse in three colors showed marked changes from totality to maximum light. This was to be expected because of the spectral types of the two components—B8 and G8 III.

At maximum the B8 star dominates and the blue deflections are greater than the other two. The yellow and ultraviolet deflections are nearly equal. During totality, the blue light decreases to less than the yellow and the ultraviolet light is almost zero.

As shown by two-color photometry in 1950 and 1951, the light-curve of the primary eclipse was unsymmetrical on the two sides. This is assumed to be caused by a stream of gas. Assuming that the up-curve is not affected by the gas and a darkening coefficient, $u = 0.4$, a ratio of the radii of the two stars, $k = 0.582$, was derived.

It is hoped that a comparison of the down-curve with the up-curve will permit a study of the character of the stream of gas. The two branches of the light-curve during the primary eclipse will be compared in the three colors directed toward a determination of the differential limb darkening. It is also hoped to observe eclipses of this star in the region of the Balmer limit.

Light-curves of primary eclipse in three colors are shown; also a plot showing the change in color, yellow minus blue and yellow minus ultraviolet.

Washburn Observatory,
University of Wisconsin,
Madison, Wis.

JACCHIA, LUIGI G. **Atmospheric fluctuations of solar origin revealed by artificial satellites.**

Atmospheric drag progessively shortens the orbital periods of artificial satellites. The decrease in period shows fluctuations which cannot be accounted for by gravitational theory. In 1957 $\beta 1$ the fluctuations were rather irregular in nature, but in 1958 $\beta 2$ and 1958 $\delta 1$ they distinctly showed the presence of 27-day cycles and were essentially synchronous. Isolated maxima and minima determined for 1958α, 1958ϵ and 1958γ indicate that also for these three satellites the fluctuations must have been in unison with the others. The rather obvious hypothesis that these fluctuations are due to a density variation of the upper atmosphere caused by variable solar radiation is confirmed by the nearly perfect parallelism of the satellite acceleration curves on one hand and the 10.7-cm solar-flux curve on the other. The relative semi-amplitude of the satellite oscillations increases with increasing perigee height, ranging from about 10 per cent for the Soviet satellites to about 35 per cent for 1958 $\beta 2$.

Another solar effect, which can be detected in 1957 $\beta 1$, 1958 $\beta 2$, and 1958 $\delta 1$ is a dependence of the orbital acceleration on the geocentric angular distance between the perigee and the subsolar point. This "diurnal" effect is not limited to the time when the perigee crosses over from night into daylight, or vice-versa, but seems to be rather a smooth function of the perigee position relative to the sun.

Smithsonian Astrophysical Observatory,
Cambridge, Mass.

McLaughlin, Dean B. **Absorption-like features in a supernova spectrum.**

The spectrum of the supernova of 1954 in NGC 4214 was studied on Lick spectrograms taken June 24 to August 19 and Mount Wilson-Palomar plates of June 6. In the blue-violet its appearance departed appreciably from that of the usual supernova spectrum of type I. Instead of the typical pattern of broad, diffuse emissions dominated by a band about λ4600, it appeared like a continuum with a few deep and several shallow absorption-like minima. Two of the strongest "absorption lines," when provisionally interpreted as λλ 4026, 4472 *He*I, give velocities near −5000 km/sec. The fainter "absorptions" are nearly all assignable to *He*I, *C*II, *O*II and *N*II with similar velocity. Deep, very broad minima near λλ 4900 and 3800 are not fully explained; otherwise the pattern of "absorption" resembles that of HD 124448 (Popper, D. M., *Pub. A. S. P.*, **58**, 370, 1946), a B-type spectrum lacking hydrogen lines. After July 8 the "absorption lines" faded. By August 19 the spectrum was that of a normal supernova of type I.

From June 6 to July 8 the supposed B-type spectrum shifted longward, the mean velocity changing from −5700 to −4700 km/sec. This suggests the hypothesis that the well-known longward shift of the blue emission bands may be due in part to decreasing shortward displacement of overlying hazy absorptions. This view encounters some difficulties. Thus, no sharpening of blue emission features accompanies the shift, and no progressive shifts occur in the red. The discrepancy between the high "absorption velocities" and the much lower expansion rate of the Crab nebula or of [*O*I] in the late stages of SN IC 4182 appears excessive. Finally, the lon persistence of a shifting but unchanging patter of absorption lines is difficult to explain in term of any model involving high-speed ejection.

The author is grateful to N. U. Mayall an R. Minkowski for the use of spectrograms, an for helpful discussions. However, this does no imply agreement with the author's interpreta tions.

The University of Michigan Observator
Ann Arbor, Mich

Oort, J. H. and Rougoor, G. W. **The inter stellar gas in the central part of the galaxy.**

The high-velocity wings of the 21-cm lin profiles in directions near that of the galacti center (Kwee *et al.* 1954) have been studie intensively in the past few years. Following ar some features of the motion and distribution o neutral hydrogen in the central region of th Galaxy following from the observations.

1) A spiral or circular arm visible from $l =$ 305° to $l = 334°$ and possibly extending t greater longitude, at $R \approx 3$ kpc, which has radial motion of about 50 km/sec directed awa from the center; at the same time it takes par in the galactic rotation with a velocity of abou 200 km/sec. The arm is seen against the con tinuous radiation of the source Sagittarius (Van Woerden *et al.* 1957). It is by far the mos regular of all the arms that have so far been ob served in the Galaxy. Its temperature is abou 100°K, the random motions average 5 km/sec i one coordinate, and the half-density thickness i the z-direction is 130 pc.

2) A spiral arm on the far side of the center broken up into bits with radial motions betwee 75 and 150 km/sec, probably also situated be tween $R = 2$ and 3 kpc.

3) A rather empty region between $R = 0.$ and 1.5 or 2 kpc.

4) A concentration within 500 pc from th center, with no radial motion and a rotationa velocity of the order of 200 km/sec. Similar hig rotational velocities close to the center hav been observed optically in some elliptical nebula and in M81.

It seems likely that the expansion is caused b magnetic fields (Oort and Rougoor 1958). Th total amount of gas moving out of the region o 3 kpc radius is roughly 1.5 solar masses per yea At this rate the central disk would be emptied i a few tens of millions of years. It seems probabl that replenishment comes from condensation o he galactic corona into the cool clouds of the isk, between $R = 1.5$ and 2.5 kpc. The magetic lines of force would then have to enter the lane at right angles and bend there to extend utward in the plane of the disk.

REFERENCES

Kwee, K. K., Muller, C. A. and Westerhout, G. 1954, *B. A. N.* **12**, 211.
Oort, J. H. and Rougoor, G. W. 1958, *Kon. Ned. Ac. Wet, Afd. Nat.* **67**, 139.
an Woerden, H., Rougoor, G. W. and Oort, J. H. 1957, *C. R. Acad. Sci. Paris* **244**, 1691.

Sterrewacht,
Leiden,
The Netherlands

Purcell, J. D., Tousey, R., Packer, D. M. and Hunter, W. R. **Solar disk photographs made with Lyman-α of hydrogen.**

A monochromatic camera for photographing he sun with the Lyman-α line of hydrogen was lown to an altitude of 200 km on March 13, 959. The instrument utilized two diffraction ratings of 40-cm radius and 600 line/mm, one eing mechanically deformed so as to produce a tigmatic image. Detailed images were obtained vith exposure times between 1 and 0.02 sec. The resolution was of the order of one-half ninute of arc. The photographs were compared vith $H\alpha$ and CaK line images taken simultaneusly by cooperating observatories. The Lyman-α mage shows intense plage areas and a general neven mottling. The resemblance is closest to he K line image, but the contrast appears reater. Several small prominences are visible.

U. S. Naval Research Laboratory,
Washington, D. C.

Sen, Hari K. and Dubs, Charles W. **A geophysical determination of the thermal electron attachment coefficient of oxygen molecules.**

The coefficient of attachment, β, of thermal lectrons to oxygen molecules in the upper part of the troposphere has been calculated using the lata from a nuclear burst at an altitude between 0,000 and 50,000 ft. Total initial gamma radiaion doses were measured at a number of points i) in the vicinity of the burst and the attenuaion of a telemetering signal from each of these oints to a ground point was measured (Haskel *t al.*). The doses and a fraction of dose rate at certain short time after burst lead to an inversequare and exponential-attenuation formula for he electron production rate. The electron denity at this time is essentially the production rate divided by the product of β and the oxygen number density; assuming a value of β, it is calculated at points along the telemetering ray path. The electron density, the electron collision frequency, and the ray frequency of nearly 225 Mc give the index of attenuation at the points. The index is numerically integrated over the ray path to give the attenuation. The value of β is chosen to make the calculated attenuations (inversely proportional to β) agree as nearly as possible with the measured attenuations.

Preliminary corrections taking into account the pressure dependence of β (2 per cent change in δ), photodetachment (5 to 15 per cent increase in δ), and absorption due to negative ions (increase in δ by a factor of 1.2 to 10) lead to the calculated values of δ in the following table:

i	Calc. δ	Exp. δ	i	Calc. δ	Exp. δ
4	2.25	5.3	10	.552	.579
5	1.83	1.85	11	.424	.367
6	1.35	1.74	13	.181	.126
7	1.23	1.51	14	.114	.0414
8	.964	1.19	15	.0752	.0438
9	.713	.821			

and to a value of K, the ratio of β divided by the oxygen number density, of $K = 7.2 \times 10^{-30}$ cm^6 sec^{-1}. This value of K is about three times that recently measured at room temperature by Chanin and Biondi (1958). It is interesting to note that the observed decrease in the echo rate of long-enduring echoes from Perseid and Arietid meteors, height approximately 80 km, leads to a value of K agreeing with ours within a factor of 2 (Kaiser 1953).

REFERENCES

Chanin and Biondi, 1958, Air Force Cambridge Research Conference, Nov. 20–21.
Haskel *et al.*, AFSWP, WT–1101, Appendix C (Confidential report).
Kaiser, T. R. 1953, *Advances in Physics* **II**, 536.

Geophysics Research Directorate,
Air Force Cambridge Research Center,
Cambridge, Mass.

Stecher, Theodore P., Johnson, Robert I. and Yoss, Kenneth M. **Spectrophotometry of RS Ophiuchi, 1958.**

The recurrent nova RS Ophiuchi had its third recorded outburst on July 14, 1958. It was observed with the Michigan instruments from July 17 through September 22. Twenty-eight spectra were obtained with the 37-inch reflector at five different dispersions, covering from λ3100 to λ8800. The identified emissions include: H, HeI, HeII, FeI, FeII, [FeII], [FeX], NI, [NII], NIII, *O* I, *O* III, *Na* I, [*A*x]. The Curtis Schmidt telescope was used with the ten-degree objective-prism combination to obtain 46 plates with a total of 65 exposures, covering from λ3600 to λ8800. Three early-type stars of suitable magnitude range were recorded simultaneously with the nova. The plates were standardized by means of a spot sensitometer, while the comparison stars were also standardized against Vega with the photoelectric monochrometer. The spectra of the comparison stars and the nova from the Schmidt plates were traced on the microphotometer and transformed into direct intensity tracings. The monochromatic intensities for the comparison stars were then combined with the corresponding photoelectric measures to give a corrected characteristic curve. The brighter nova emission-line intensities were then expressed in terms of the Code-Whitford monochromatic magnitudes for Vega.

The University of Michigan Observatory,
Ann Arbor, Mich.
Louisiana State University,
Baton Rouge, La.

STEPHENSON, C. B. **Visual binaries having primaries above the main sequence.**

Magnitudes and MK spectral types for both components of more than 150 physical visual binaries having primaries above the main sequence have been used in the consideration of a number of problems. More than two-thirds of the spectroscopic data were newly obtained with the 36-inch refractor of the Lick Observatory, and some new photometric data were derived.

The more interesting conclusions concerning or drawn from such binaries are the following. 1) There is no correlation, or at most a weak one, between the nature of the members of a fairly wide binary and their mean separation. 2) The frequency distribution of separations for giant-primary systems is similar to that derived by Kuiper many years ago for dwarfs. 3) The distribution of components of double stars in the H-R diagram is consistent with a scheme of evolution in which stars leave the main sequence in order of decreasing mass, and, initially, follow paths which do not carry them below their starting points either bolometrically or visually. Further support is found for the idea that late-type giants and subgiants are commonly very old. 4) The existing luminosity calibration for stars of type G5 and later and of luminosity class II and fainter is substantially correct, except for luminosity class II. 5) The uncertainty in visual absolute magnitude associated with the assignment of a given luminosity class of II or fainter to stars of most spectral types is represented by a standard deviation of about half a magnitude. There are no preferred luminosities above the main sequence for stars of the general field, except among the late-type giants. 6) The dynamical parallaxes that have been published for the wider visual binaries are probably based on larger than average relative motions, and hence these motions are unsuitable for deduction of mean stellar masses.

Warner and Swasey Observatory,
Case Institute of Technology,
Cleveland, Ohio

STOCK, J. AND NASSAU, J. J. **Objective prism surveys of stars of high luminosity.**

This report deals with the use of the ultraviolet spectral region for the detection of stars of high luminosity. Plates taken with the large Schmidt-type telescope of the Hamburg Observatory equipped with a UV objective prism were used for the purpose. With such spectra it is possible to identify and for certain types to classify highly luminous stars from OB to G0. The criteria employed are:

a) For the OB group the absolute strength of the hydrogen line is used. It is possible to segregate from this group stars with the Balmer continuum in emission. The majority of such stars are expected to be of lower luminosity than that indicated by their absorption-line intensity.

b) For stars from about B6 to G0, temperature and luminosity criteria may be secured from the Balmer jump, the absorption of the Balmer lines, and the strength of the H and K lines and the G-band.

For most of the spectral classes given above it is possible to reach about the 13th magnitude. In view of this it was thought profitable to initiate a survey covering the complete sky.

The Hamburg and Case Observatories are participating in this project. A suitable prism for this purpose for the Cleveland observatory has been made available by a grant from the National Science Foundation. It is hoped that the Boyden Observatory will participate in the survey for the southern sky.

A region of 600 square degrees in Cassiopeia and Perseus has been surveyed at Hamburg and the results are nearly ready for publication.

About 1900 stars of high luminosity were found in this area of which 1633 stars were OB and 261 were of the later-type supergiants. About 25 per cent of the stars of magnitude 12 and brighter show the ultraviolet emission. The surface distribution of these luminous stars seems to indicate that the relative frequency of the different types differs from association to association.

An area of similar size in Sagitta, Vulpecula and Cygnus has been surveyed in Cleveland with plates taken at Hamburg. The total number of highly luminous stars in this region is about 1000 with a conspicuous concentration in the P Cygni area. The percentage of stars showing the ultraviolet emission is about the same. It was also noted that the later-type supergiants do not show the same concentration around the P Cygni region as the OB stars.

Warner and Swasey Observatory,
Case Institute of Technology,
Cleveland, Ohio

Stock, J. and Upgren, A. R., Jr. **Characteristics of objective prisms.**

Certain characteristics of objective prisms such as the variation of the dispersion across the field and the field distortions on the plate caused by the prism have been investigated on a theoretical basis.

For spectrophotometric programs it is preferred that the dispersion vary as little as possible across the field while for survey programs it s advantageous for the field distortion to be minimized in order that the positions of the stars may be measured conveniently directly from the spectral plates themselves.

For a prism of given angle and index of refraction, it has been shown that the variation of dispersion and the field distortion depend upon the angle between the prism and the optical axis of the telescope. It was found that the dispersion varies least for a value of this angle different from that for the case of minimum deflection. The field distortions, although minimized for the value of the angle corresponding to minimum deflection, are only slightly larger and are of a simpler form with the value of the angle corresponding to minimum dispersion.

It seems desirable, therefore, to mount an obective prism at the angle for which the dispersion is a minimum rather than at the angle for minimum deflection as has often been done.

Warner and Swasey Observatory,
Case Institute of Technology,
Cleveland, Ohio

Swihart, Thomas L. **Convection in the sun.**

It is well known that a radiative model of the solar atmosphere has a negative density gradient in the moderately deep layers. The minimum convection in the sun would thus be that amount which would remove this negative gradient. The maximum convection would be found by using the adiabatic temperature gradient in the unstable layers.

The above described atmospheres, as well as a purely radiative atmosphere, were constructed on the Los Alamos IBM 704 calculator, and the resulting radiation fields were compared with observations. The adiabatic model was considerably superior to the other two in reproducing observed limb-darkening values and the resulting temperature-optical depth relation, and it was also somewhat better in reproducing absolute monochromatic intensities at the center of the disc; however it predicted a Balmer discontinuity of only 0.06, while the minimum convective and the radiative models had 0.08 and 0.11 respectively.

Instability according to the Schwarzschild criterion sets in at an optical depth ($\lambda 5000$) of 0.8 for the adiabatic model and about 1.1 for the minimum convective model.

Los Alamos Scientific Laboratory,
University of California,
Los Alamos, N. M.

Tousey, R., Purcell, J. D., Packer, D. M. and Hunter, W. R. **A new solar spectrum in the extreme ultraviolet.**

An extreme ultraviolet spectrograph, employing near normal incidence a grating of 40-cm radius and 600 line/mm, was flown to an altitude of 200 km on March 13, 1959. This spectrograph was greatly improved in speed and straylight characteristics through the use of an aluminum oxide over germanium coating on the plastic grating surface. Approximately 100 emission lines were photographed, with a resolution of about 1/2Å. The first 11 lines of the Lyman series were resolved, except for γ, which was not positively present, presumably because of extremely strong absorption by O_2. Below 919Å a rise in background density takes place, reaching a maximum at 910Å, then falling gradually to the straylight level at about 850Å. This may be ascribable to the unresolved high members of the Lyman series and the Lyman continuum. Among new lines identified at this time are *He*I 584.3Å, *O*II and *O*III resonance lines near 834Å, *O*IV 788, 790 and 608, 610Å, and *Mg*X, 625Å. The strongest of the resonance lines of neutral and excited nitrogen were found, but their intensities were comparatively low. These include *N*I 1199.5, 1200.2, 1200.7Å; *M*II, five lines unresolved near 1085Å; *N*III 989.8, 991.5Å. A line present at 1036Å on the shoulder of *O*VI 1037.6Å may be the resonance line of *Be*II 1036.3Å, but there is the possibility of a blend with *C*II 1036.3, 1037.0Å. The *Ne*I 735.9Å line was not detected.

U. S. Naval Research Laboratory,
Washington, D. C.

UNDERHILL, ANNE B. **Line Shapes in the Wolf-Rayet Stars HD 192103 and HD 192163.**

Profiles of the emission *He*II lines λ4686 (3–4), λ3203 (3–5), and λ5411 (4–7) have been derived from plates of moderate dispersion for HD 192103, WC7, and for HD 192163, WN6. None of these lines is severely distorted by blending, although there is some blending with the wings of λ4686 in the case of HD 192103.

The profiles of λ4686 and λ3203 are similar for each star, consisting of a rounded core of Gaussian shape, and weak wings. The core of λ5411 in each case is similar in intensity and shape to that of λ3203, but there are no appreciable wings. The lines of the 5-n series from λ6583 (5–13) to λ6074 (5–20) appear on the spectrograms. These lines are weak, but they seem to have the same shape as the well-determined profiles of λ4686, λ3203 and λ5411. The total half-width of the *He*II emission lines is about 1300 km/sec in HD 192103 and about 2000 km/sec in HD 192163. There is no evidence of any displaced absorption components even for the very strong λ4686 line.

These data supprt the hypothesis that the shapes of the emission lines in Wolf-Rayet stars are chiefly determined by large chaotic motions of the emitting gases. The hypothesis of Stark broadening is untenable, for if this agent were active the high series members should be broader than λ4686 and λ3203, which they are not. Electron scattering probably is not very important, else λ5411 should have wings as strong as those of λ3203. The hypothesis of a rapidly expanding shell is of doubtful validity because the intrinsically strong line λ4686 does not have a displaced absorption component. The weak wings of λ4686 and of λ3203 become prominent with respect to the core because the cores of these lines are probably weakened by self-absorption.

Displaced absorption lines of *He*I, *C*III and *N*IV are present. Only those spectral transitions are observed in absorption which arise fror levels which will be overpopulated in a dilute radiation field at high electron temperatur that is transitions from the 3_s and 3_p levels i the case of *He*I. The streaming velocity −1100 km/sec in the case of HD 192103 an −1400 km/sec in the case of HD 192163. It concluded that the quasi-stable emitting regio visible in the *He*II emission lines is surrounde by a low density gas which is streaming from th star.

The profile of *C*III λ5696 in HD 192103 is th only flat-topped emission feature in this W spectrum. The total half-width of this line 2000 km/sec, and there may be some structu in the profile. This line makes visible both velo ity fields: (i) the quasi-stable atmosphere whe a recombination emission spectrum is forme (*He*II lines etc.), and (ii) the low density strea ing atmosphere observed in the absorption line This *C*III line may be formed by two processe (i) recombination and (ii) as a result of a cyc involving *He*II λ303 quanta in a low density g which contains C^+ ions (Underhill, A. B., *Ap.* **126**, 28, 1957). The emission arising from t latter process widens the line because of t motion of the C^+ ions and may produce structu on the smooth profile of the recombination lin

Dominion Astrophysical Observato
Victoria, B.

WESTERHOUT, GART. **Recent galactic and extr galactic studies at Dwingeloo, The Nethe lands.**

The 25-meter radio telescope at Dwingelo in continuous use now for over 2½ years, h proved an excellent tool for detailed studies the Galaxy and extragalactic systems.

Results of an investigation of the central r gions of the Galaxy are presented in anoth paper. Further 21-cm line investigations inclu a region of the Galaxy between $R = 3.5$ and kpc, the Orion region, the association II Mon cerotis, regions in Perseus, and six extragalact nebulae.

A large number of line profiles and drift curv are being obtained between $l = 350°$ and 10 $b \doteq +10°$ to $-10°$, in order to investiga whether the expansion of the neutral hydrog in the central parts of the Galaxy continu further outward. The ultimate aim of this i vestigation is a better value of the rotation velocity between $R = 3.5$ and 6 kpc, and a mo detailed resolution of the spiral structure.

In the Orion region, the work done at Harvard is being repeated in more detail and in a larger region. Detailed correlation is found between dark clouds and intensity of 21-cm line radiation.

In Perseus, individual clouds have been found at over 1000 pc from the galactic plane. The extragalactic nebulae M33, M101, M81, IC 1613, NGC 6822 and NGC 4236 have been investigated in detail in a similar manner as M31 (Van de Hulst *et al.* 1957; Raimond and Volders 1957). The density distribution and rotation in M33 and M101 could be derived, from which it was possible to find the total amount of hydrogen ($10^9\ M_\odot$ and $3 \times 10^9\ M_\odot$) and the total mass ($18 \times 10^9\ M_\odot$ and $140 \times 10^9\ M_\odot$). The irregular nebula NGC 6822 is also rather bright, while the radiation from M81, IC 1613 and NGC 4236 is very faint. The hydrogen content of irregular nebulae is much higher than that of regular types.

From a survey of the continuous radiation at 22 cm, the gross distribution of ionized hydrogen throughout the Galaxy was derived (Westerhout 1958). The total mass of ionized hydrogen is of the order of $4 \times 10^7\ M_\odot$. Values of the emission measure of many emission nebulae could be determined.

A survey of the continuous radiation at 75 cm is partly reduced, and shows many interesting details in the Milky Way and the galactic corona.

REFERENCES

Raimond, E. and Volders, L. M. J. S. 1957, *B. A. N.* **14**, 19.
van de Hulst, H. C., Raimond, E. and van Woerden, H. 1957, *B. A. N.* **14**, 1.
Westerhout, G. 1958, *B. A. N.* **14**, 215 and 261.

Sterrewacht,
Leiden,
The Netherlands

WILSON, RAYMOND H., JR. Magnetic damping of rotation of satellite 1958 $\beta 2$.

The rotation rate of artificial satellite Vanguard I (1958 $\beta 2$) has been measured almost daily for nearly a year by observing the frequency of radio signal maxima due to passages of the satellite's dipole-antenna lobes across ground-receiving stations. The spin rate is thus observed to decay exponentially with elapsed time, as represented by an equation of the form reported to this Society three years ago (Wilson, R., *A. J.* **61**, 193, 1956). The constants for this equation which depend on the physical characteristics of the satellite, such as moment of inertia, electrical conductivity, and magnetic permeability, have been determined experimentally. The resulting relation indicates an effective mean magnetic field component perpendicular to the spin axis which is consistent with reasonable assumptions of the magnetic orientation of the axis in the known field of the earth.

Vanguard Division,
National Aeronautics and Space Administration,
Washington, D. C.

TITLES OF ADDITIONAL PAPERS

- BECKER, ROBERT A. Possibility of anomalous abundance ratio of elements produced by rapid neutron-capture in supernovae.
- BLANCO, V. M. AND WILLIAMS, A. D. An O-B association with an unusual color effect.
- BONSACK, WALTER K. The abundance of lithium and internal convection in K stars.
- BURBIDGE, E. MARGARET, BURBIDGE, G. R. AND PRENDERGAST, K. H. Mass distribution and physical conditions in the inner region of NGC 1068.
- BURBIDGE, G. R. AND BURBIDGE, E. MARGARET. The Hercules cluster of galaxies.
- COOK, ALLAN F. II AND HAWKINS, GERALD S. The meteoric head echo.
- DE VAUCOULEURS, G. Photographic diameters of bright galaxies.
- FITCH, W. S. Overtone pulsations of CC Andromedae and the short-period variables.
- HOWARD, ROBERT F. Observations of solar magnetic fields.
- JEFFERIES, J. T. AND ORRALL, F. Q. The empirical determination of Balmer-line source functions.
- JEFFERIES, J. T. AND THOMAS, R. N. The width of Ca^+ emission cores.
- JONES, R. CLARK. Quantum efficiency of photographic films.
- KIESS, C. C., CORLISS, C. H. AND KIESS, HARRIET K. High-dispersion spectra of Jupiter.
- KRAFT, ROBERT B. AND GREENSTEIN, JESSE L. The binary system Nova DQ Herculis: I. The spectrum and radial velocity during the eclipse cycle.
- KRAFT, ROBERT B. The binary system Nova DQ Herculis: II. An interpretation of the spectrum during the eclipse cycle.
- MAXWELL, A. The four spectral types of solar radio bursts.
- MAXWELL, A., THOMPSON, A. R. AND GARMIRE, G. The association of cosmic rays and auroral streams with solar radio bursts.
- MCCROSKY, R. E. Observations of simulated meteors at 80 kilometers.
- MCCUSKEY, SIDNEY, W. The giant-dwarf ratio among the G5 stars.
- O'KEEFE, JOHN A., ECKELS, D. ANN AND SQUIRES, R. KENNETH. Contribution to the theory of the Vanguard satellite.
- POTTASCH, S. R. AND THOMAS, R. N. Non-LTE effects under high opacity in the Lyman continuum.
- ROACH, F. E. The absolute brightness of nightglow [*O*I] 5577 at the geomagnetic pole.
- SAVEDOFF, M. P. AND VAN DYCK, S. Stellar evolution at mass 10.
- SMITH, STEPHEN J. AND BURCH, DAVID S. Experimental determination of the bound-free absorption coefficient of H^-.
- SWARUP, G., STONE, P. H. AND MAXWELL, A. Association between solar spectral radio bursts and solar flares and prominences.
- VAN DEN BERGH, SIDNEY. Dwarf galaxies.
- VAN DE KAMP, PETER. Parallax and orbital motion of L726-8.
- WHIPPLE, FRED L. On the distribution of semi-major axes among comet orbits.

PARTICLE TRAJECTORIES AROUND CLOSE BINARY SYSTEMS

By NANCY L. GOULD
Berkeley Astronomical Department, University of California

Received June 16, 1958

Abstract. The differential equations of motion for the restricted three-body problem have been integrated numericall to give the path (in a rotating frame of reference) of a particle ejected radially from one component of a close doub star system. This has been done for several mass ratios and initial positions and velocities. The most usual results a a ring around one component rotating in a forward direction, or for higher velocities, a ring around both componen rotating in a retrograde direction. A particle ejected from the first Lagrangian point will form an orbit only if the ma of the star from which it is ejected is approximately one-fifth or less that of its companion.

When a particle is ejected from one component of a close binary system its motion, under the influence of gravity, is described by the differential equations of the classic *problème restreint.* In the hope of shedding some light on the behavior which might be expected of gas streams in close binary systems a number of integrations of these equations were made for a variety of mass ratios, initial positions and velocities. The integrations were performed on the University of California's IBM 701 electronic computer at Berkeley. Details of the calculations and preliminary results have been given in an earlier report (Gould 1957). Since then more integrations have been carried out and plotted, and some aspects of an overall picture emerge.

The early investigators (Darwin 1897; Moulton 1920; Strömgren 1922) of the problem concerned themselves almost exclusively with the search for periodic solutions. No such attempt was made in the present instance and none of the strictly periodic solutions were encountered. However in some cases a particle rotating in a forward direction around the primary component may continue indefinitely.

Kopal's (1956) more recent investigation is of the same type as the present one, except that he considers ejection from L_1 at an angle to the line of centers of the two stars, whereas I am concerned with radial ejection only.

A number of cases were studied in which a particle was ejected at the first Lagrangian point directly towards the opposite component. These included ejection both from the primary (more massive) and from the secondary components. In all of the cases considered here the unit of velocity is the relative circular velocity of the system. It was found that unless the star from which the material is ejected had a mass approximately one-fifth (or less) that of its companion, the material would go directly to it, falling in on its following face, as in Figure 1. This is true for all velocities and any combination of masse except as noted above. Ejection from a second ary in a system with a mass ratio of 0.2 (μ 0.167) produces paths such as are shown i Figures 2 and 3.

If the particles are ejected from a point interio to L_1 on the line of centers of the two stars som interesting trajectories may be formed. This i of course, because the coriolis force has so change the direction of the particle by the time it reache the inner zero velocity surface that it never passe through L_1 traveling directly along the x-axi Integrations of this type were made for severa mass ratios and initial velocities. Figures 4, 5, 7 and 8 show ejection from the secondary, Fig ures 9 and 10 ejection from the primary. Agai there seems to be no dichotomy between ejectio from primary or secondary. The general tenc ency is for the particle to form a ring around th opposite component rotating in a forward dire tion. As the initial velocity is increased there a stronger and stronger tendency for the partic to reverse its direction in the neighborhood L_3 and form a considerably larger ring aroun both components rotating in a retrograde dire tion. As the mass ratio is increased the effect the same as an increase in the initial velocity fo a single mass ratio. Consequently ejection fro the primary is much less likely to form a rir around the secondary than vice versa.

The last group of cases to be considered he are those in which particles are ejected radiall around the equator of the secondary, not merel towards the primary. These are illustrated Figures 11 through 15. The general pattern whic emerges is this: there is a rather sharply define minimum velocity below which the particl simply fall back. At slightly greater initial veloc ties a ring is formed around the primary, rotatir in a forward direction. As the velocity increas still more there is a greater and greater tendenc for the particles to pass over the receding fa

Fig. 1

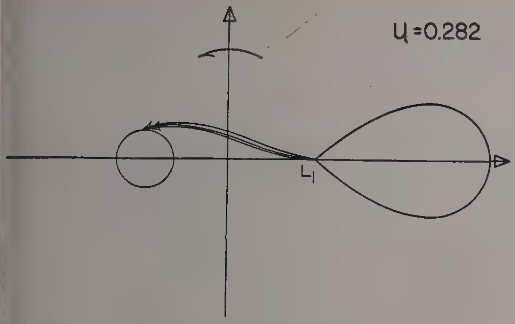

Fig. 2

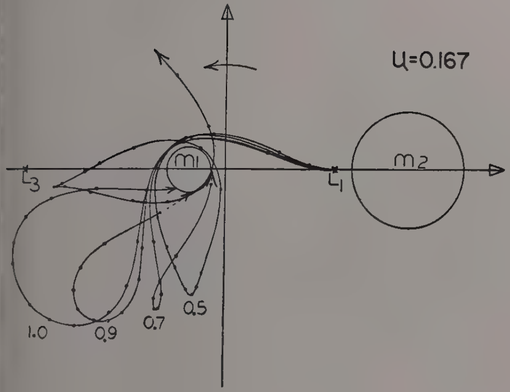

Fig. 3

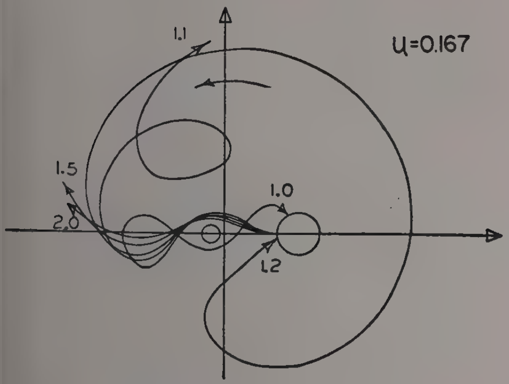

Figure 1. Ejection from secondary at L₁. $\mu = 0.282$. Initial velocities from 0.05 to 5.0.

Figure 2. Ejection from secondary at L₁. $\mu = 0.167$. $(m_2/m_1 = 0.2.)$ $v_0 = 0.5, 0.7, 0.9, 1.0$.

Figure 3. Ejection from secondary at L₁. $\mu = 0.167$. $v_0 = 1.0, 1.1, 1.2, 1.5, 2.0$.

Fig. 4

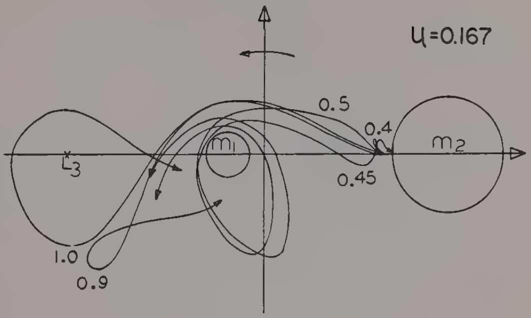

Fig. 5

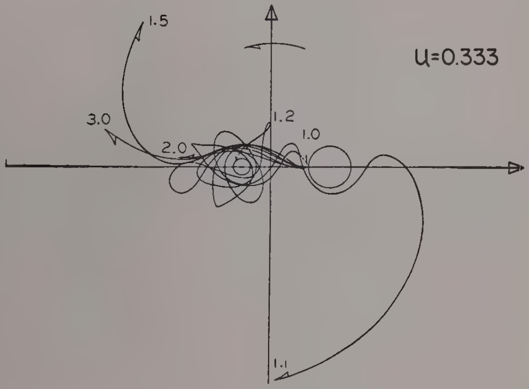

Fig. 6

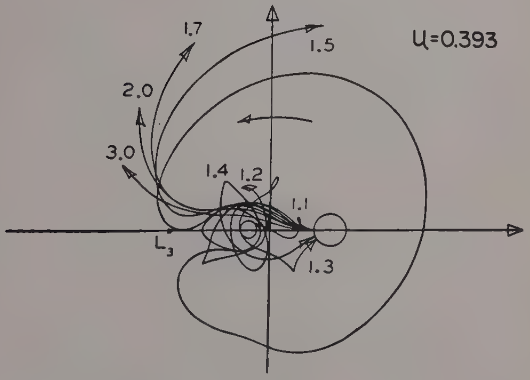

Figure 4. Ejection from secondary at surface of round star. $\mu = 0.167$. $v_0 = 0.4, 0.45, 0.5, 0.9, 1.0$.

Figure 5. Ejection from secondary at surface of round star. $\mu = 0.333$. $v_0 = 1.0, 1.1, 1.2, 1.5, 2.0, 3.0$.

Figure 6. Ejection from surface of round secondary. $\mu = 0.393$. $v_0 = 1.1, 1.2, 1.4, 1.5, 1.7, 2.0\ 3.0$.

Fig.7

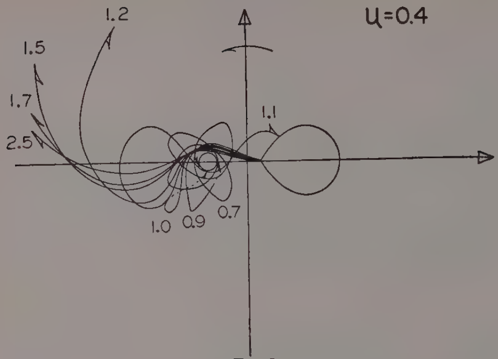

Fig.8

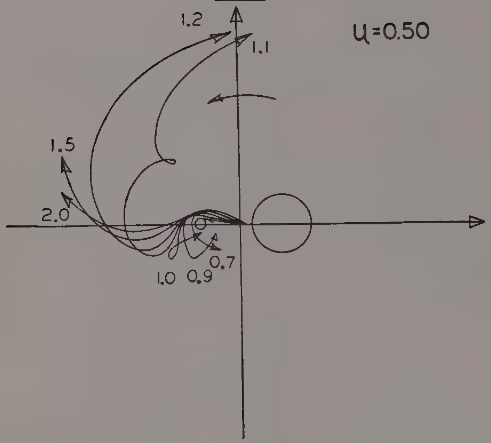

Fig.9

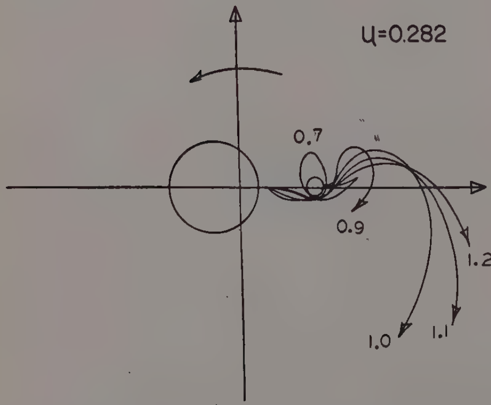

Figure 7. Ejection from surface of round secondary. $\mu = 0.4$. $v_0 = 0.7, 0.9, 1.0, 1.1, 1.2, 1.5, 1.7, 2.5$.

Figure 8. Ejection from surface of round secondary. $\mu = 0.5$. $v_0 = 0.7, 0.9, 1.0, 1.1, 1.2, 1.5, 2.0$.

Figure 9. Ejection from surface of round primary. $\mu = 0.282$. $v_0 = 0.7, 0.9, 1.0, 1.1, 1.2$.

Fig.10

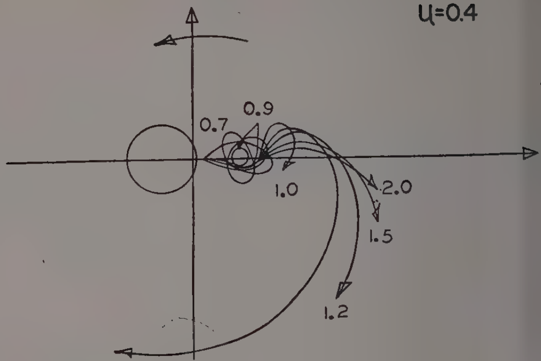

Fig.11

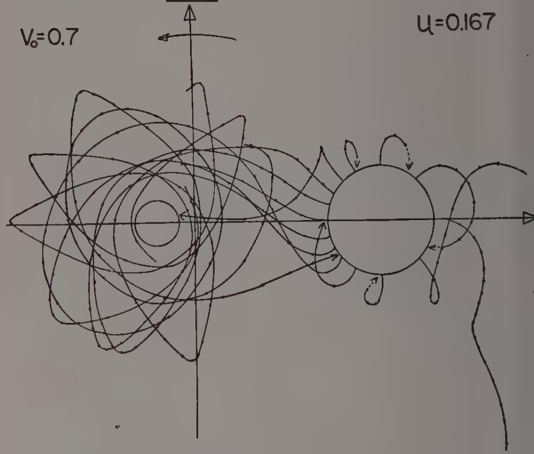

Fig.12

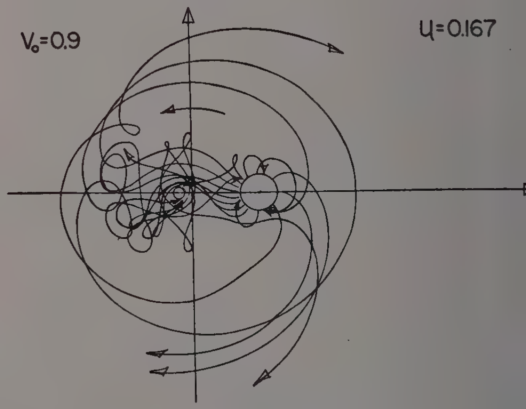

Figure 10. Ejection from surface of round primary. $\mu = 0.4$. $v_0 = 0.7, 0.9, 1.0, 1.1, 1.2, 1.5, 2.0$.

Figure 11. Ejection from points around equator of secondary. $\mu = 0.4$. $v_0 = 0.7$.

Figure 12. Ejection from points around equator of secondary. $\mu = 0.167$. $v_0 = 0.9$.

Fig. 13

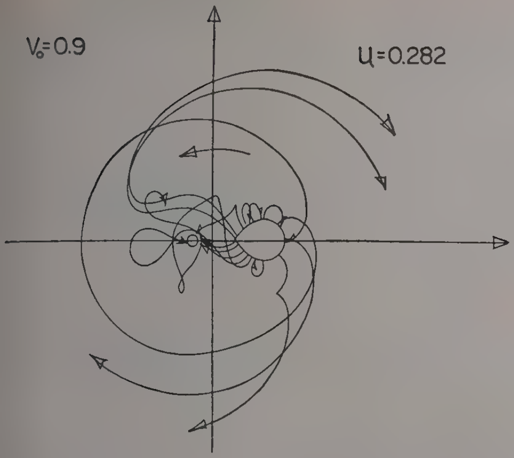

Fig. 14

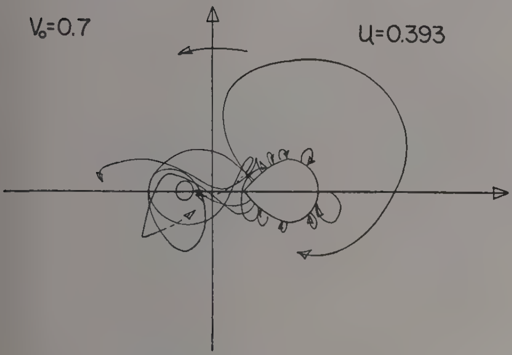

Figure 13. Ejection from points around equator of secondary. $\mu = 0.282$. $v_0 = 0.9$.

Figure 14. Ejection from points around equator of secondary. $\mu = 0.393$. $v_0 = 0.7$.

Fig. 15

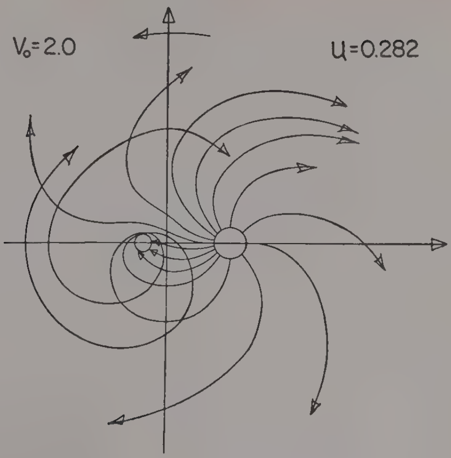

Figure 15. Ejection from points around equator of secondary for very high velocity. $\mu = 0.282$. $v_0 = 2.0$.

of the primary, reverse their direction in the vicinity of L_3 and form a ring or outward spiral around the entire system with a retrograde motion. As the mass ratio increases the activity is concentrated more and more on the hemisphere facing the more massive star. For a very high initial velocity, for example two times the rotational velocity of the system, there is a sort of pinwheel effect.

As a result of these integrations certain effects seem probable:

1. A concentration of matter between the stars which favors the following hemisphere of the opposite component from which it was ejected.
2. A ring rotating in a forward direction will be around one component only and relatively small. Under certain conditions this ring may be larger and denser on the approaching hemisphere.
3. A ring rotating in a retrograde direction will be around both components, be considerably larger, and be formed as a result of generally higher initial velocities and mass ratios.
4. A concentration of matter at the third Lagrangian point only in the sense that it is in this vicinity that a particle may pause as it changes its direction from direct to retrograde.
5. No clear-cut difference between ejection from the primary and from the secondary, but rather a gradual progression with mass ratio.
6. Ejection from the first Lagrangian point will form an orbit only if the star from which it is ejected has a mass of approximately one-fifth, or less, that of its companion.

Many of the results were plotted automatically with equipment belonging to the University of California Radiation Laboratory at Livermore. I am indebted to Mrs. Diana Lees for the use of a differential equation program and for much assistance. The computations on the 701 were partially supported by the National Science Foundation.

REFERENCES

Darwin, G. H. 1897, *Acta Math.* **21**, 99.
Gould, Nancy L. 1957, *Pub. A. S. P.* **69**, 541.
Kopal, Z. 1956, *Annales d'Astrophysique* **19**, 298.
Moulton, F. R. 1920, *Periodic Orbits*, Carnegie Publication 161 (Washington).
Strömgren, E. 1922, *Publikationer og mindre Meddeleser fra Kobenhavn Observatorium*, Nr. 39.

INEQUALITIES IN MEAN SOLAR TIME FROM TIDAL VARIATIONS IN THE ROTATION OF THE EARTH

By EDGAR W. WOOLARD
U. S. Naval Observatory, Washington, D. C.

Received February 27, 1959

Abstract. The deformation of the earth by the luni-solar tide-generating forces alters the moments of inertia of the earth and thereby causes periodic variations in the rate of rotation, which introduce inequalities in the measure of time determined by the rotation. The cumulative effects of the larger long-period components with periods up to one year have been detected by observation with the aid of accurate clocks. In this paper, all long-period inequalities with amplitudes as great as 0.10 millisecond are computed, and are listed in Table I.

Some inequalities in the rate of rotation of the earth are due to variations of the moments of inertia, caused by the deformations of the earth by the luni-solar tide-generating forces. In order to determine these inequalities only the principal term of the expansion of the tide-generating potential in powers of the parallax of the tide-producing body need be considered. At a point on the earth where the radius is ρ and the intensity of gravity is g, this term of the tidal potential for the action of a body of mass M and parallax π, when at zenith distance z, is

$$U = g\left\{\frac{3}{2}\frac{M}{E}\rho\sin^3\pi\left(\cos z - \frac{1}{3}\right)\right\},$$

in which E denotes the mass of the earth. The tides from the terms of higher order are hardly appreciable, and their effects on the rotation of the earth are completely insensible.

We may anticipate that only deformations by long-period forces will produce cumulative effects on the rotation that are sufficiently large and regular to cause observable inequalities in the measure of time determined by the rotation. These deformations may reasonably be expected to conform closely to the equilibrium theory.

By expressing z in terms of the declination δ and the hour angle of M, the long-period component of the potential, independent of the hour angle, is found to be

$$U_0 = g\frac{3}{2}\frac{M}{E}\left(\frac{a_0}{a}\right)^3 a_0\left(\frac{1}{2}-\frac{3}{2}\sin^2\varphi'\right) \times\left\{\left(\frac{a}{r}\right)^3\left(\frac{1}{3}-\sin^2\delta\right)\right\},$$

in which a_0 is the mean radius of the earth, φ' the geocentric latitude, r the geocentric distance of M, and a the mean distance; with sufficient accuracy, $g = G(E/a_0^2)$, where G is the constant of gravitation.

On the hypothesis that the deformation of the earth conforms to the equilibrium theory, the radial deformation $\Delta\rho$ of the surface is a fraction k of the amount U_0/g by which the level of the equipotential surface of gravity is elevated by the additional potential U_0. The value of the parameter k depends upon the mechanical properties of the earth as a whole, particularly upon whether the yielding under stress is elastic or plastic.

At the surface of the earth, therefore, as a result of the tidal deformation, $\Delta\rho = k(U_0/g)$, the gravity potential changes by an amount kU_0. This change is due to the change in the gravitational potential V of the earth brought about by the redistribution of mass in the deformation; its amount $\Delta V = kU_0$ may be determined with sufficient accuracy from the expression for the external potential of a concentrically homogeneous spheroid of revolution with principal moments of inertia $A = B < C$, by differentiating with respect to these moments. At distance R from the center of mass, to the third order in a_0/R,

$$V = G\frac{E}{R} + G\frac{C-A}{R^3}\left(\frac{1}{2}-\frac{3}{2}\sin^2\varphi'\right).$$

Neglecting compressibility, $\Delta A + \Delta B + \Delta C = 0$, from which, in ΔV,

$$\Delta(C-A) = \frac{3}{2}\Delta C,$$

and at the surface, where $R = a_0$, equating ΔV to kU_0 gives

$$\frac{\Delta C}{C} = k\frac{Ea_0^2}{C}\frac{M}{E}\left(\frac{a_0}{a}\right)^3\left\{\left(\frac{a}{r}\right)^3\left(\frac{1}{3}-\sin^2\delta\right)\right\}.$$

The factor Ea_0^2/C may be evaluated from its relation to the flattening of the earth, f, and the ratio m of the centripetal acceleration of rotation at the equator to gravity,

$$\frac{3}{2}\frac{C-A}{Ea_0^2} = f - \tfrac{1}{2}m;$$

th $f = 1/297$, $m = 1/288.4$, and $(C - A)/C =$ 305.6, this relation, which depends only upon e condition that the surface is an ellipsoid of volution in equilibrium with gravity, gives ${}_0^2/C = 3.00$.

Since the axis of C is so nearly the axis of tation, the angular momentum is virtually $C\omega$, d from the condition that $C\omega =$ const., the riation of the moment of inertia causes a varia-on in the rate of rotation ω according to the lation

$$\Delta C/C = -\Delta\omega/\omega.$$

decrease $-\Delta\omega$ in the rate of rotation per day uses the length t of the day to increase by an nount Δt per day; therefore

$$-\Delta\omega/\omega = \Delta t/t,$$

which Δt is the amount per day that a perfect ock would *gain* on mean solar time. The accu-ulated departure of a uniformly running clock om mean solar time at any instant t is $\int_0^t \Delta t\,dt$.

hen obtaining the clock correction on each ght by observation, no allowance is made for is difference. Consequently, the clock *correc-ms* contain the *negative* of the tidal inequality mean time.

From the expression for $\Delta C/C$, the daily gain a uniform clock on mean solar time, due to the ng-period component of the principal equilib-um tide, is

$$\begin{aligned} &= k\frac{3M}{E}\left(\frac{a_0}{a}\right)^3\left\{\left(\frac{a}{r}\right)^3\left(\frac{1}{3}-\sin^2\delta\right)\right\} \\ &= k\frac{3M}{E}\left(\frac{a_0}{a}\right)^3\left\{\frac{1}{3}\left(\frac{a}{r}\right)^3\right. \\ &\qquad - \cos^2\epsilon\left(\frac{a}{r}\right)^3\sin^2\beta \\ &\qquad - \sin^2\epsilon\left(\frac{a}{r}\right)^3\cos^2\beta\sin^2\lambda \\ &\qquad \left. - \sin 2\epsilon\left(\frac{a}{r}\right)^3\cos\beta\sin\beta\sin\lambda\right\}, \end{aligned}$$

here λ and β are the celestial longitude and titude of M, and ϵ is the obliquity of the cliptic.

In order to integrate this expression, it is ex-anded in series which may be immediately ob-ined from the developments given by Woolard 953) in Tables 11, 15, 16, 19, and 21 of his aper on the rotational motion of the earth; the tegrating factors are obtained from Table 23. From among the terms in each of the tables, the particular ones are taken that are necessary to obtain whatever order of accuracy is desired after terms with like arguments from the different tables are added and the series is integrated. The expansion may be checked with the development of the tidal potential derived by Doodson (1921) in a different way.

The value of the common constant coefficient in the series for Δt, with the day as the unit of time, is

$$\begin{array}{lcc} & \text{Moon} & \text{Sun} \\ k(3M/E)(a_0/a)^3t = & 0\overset{\mathrm{s}}{.}014524\,k & 0\overset{\mathrm{s}}{.}006630\,k. \end{array}$$

The exact value of k is still uncertain.

Table I gives the expression for the accumulated gain of a uniform clock on mean time at any instant, inclusive of all terms with coefficients which, for any probable value of k, will be as great as 0.10 millisecond. The lunar fortnightly and solar semiannual terms, and the term in ☊, have been derived by several previous writers in various ways (Melchior 1957).

TABLE I. DEPARTURE OF A UNIFORM CLOCK FROM NON-SMOOTHED MEAN SOLAR TIME, *clock − mean*, DUE TO TIDAL VARIATIONS IN THE ROTATION OF THE EARTH

Coefficient of sine	Argument	Period
$+0\overset{\mathrm{s}}{.}00032\,k$	2L + *g*	$9\overset{\mathrm{d}}{.}1$
$+\quad 13\,k$	2L + *g* − ☊	
$+0.00247\,k$	2L	13.7
$+\quad 102\,k$	2L − ☊	
$+\quad 10\,k$	2L − 2☊	
$+0.00011\,k$	2*g*	13.8
$+0.00023\,k$	2L − 2⊙	14.8
$+0.00263\,k$	*g*	27.6
$-\quad 17\,k$	*g* + ☊	
$-\quad 17\,k$	*g* − ☊	
$-0.00014\,k$	2L − *g*	27.1
$-\quad 6\,k$	2L − *g* − ☊	
$+0.00058\,k$	2L − *g* − 2⊙	31.8
$+0.00060\,k$	2⊙ + *g′*	122
$+0.01529\,k$	2⊙	183
$-\quad 37\,k$	2⊙ − ☊	
$+0.00488\,k$	*g′*	365
$-0.00023\,k$	2⊙ − *g′*	365^{d}
$+0.5150\,k$	☊	$18\overset{\mathrm{y}}{.}6$
$-\quad 27\,k$	2☊	9.3

L—Mean longitude of the moon.
g—Mean anomaly of the moon.
☊—Mean longitude of the ascending lunar node.
⊙—Mean longitude of the sun.
g′—Mean anomaly of the sun.

The coefficient of each term is the maximum amount of the clock departure, and is half the total variation from the maximum positive value to the maximum negative value which occurs during every half-period; the rate of departure Δt is alternately positive and negative, and the gain or loss continually accumulates for half of the period.

The expression for Δt before it is expanded in series shows that the rate depends upon the declination. The clock departure due to the lunar tide will therefore vary with the declination of the moon during each monthly revolution. In Table I, this dependence on declination is represented by the terms that contain ☊ in the argument. The monthly range in declination is determined by the position of the node; terms with arguments that differ only by a multiple of ☊ may be combined into a single term having a variable coefficient that contains ☊, and this more direct representation is the usual practice in tidal theory.

The range in declination is not the same every month, but continually changes during the period of 18.6 years in which the nodes regress through a complete circuit of the ecliptic. Consequently the alternate increase and decrease of ω each month from the fortnightly and monthly tide do not completely compensate for each other and the residual accumulates for more than years, producing the 18.6-year term with argument ☊ in Table I. During the years when ☊ i near 180°, the moon remains relatively near the equator, and on the average the tidal deformation increases the flattening of the earth slightly increasing C and decreasing ω. Because of the great length of the period during which the effec continually accumulates in one direction, the amplitude of the inequality in the clock departure is very large; but clocks have not yet kep time over sufficiently long intervals with the accuracy necessary to separate this variation from the variations of the clock. However, i might possibly be detected by harmonic analysis of sufficiently accurate values of the lunar fluctuation extending over a long enough interva of years.

REFERENCES

Doodson, A. T. 1921, *Proc. Roy. Soc.* A **100**, 305.
Melchior, P. J. 1957, *Bull. Géod.* No. **46**, 47.
Woolard, E. W. 1953, *Astr. Papers Amer. Ephemeris* **XV**,

TABLES OF SECULAR PERTURBATIONS OF SHORT PERIOD ORBITS

By S. E. HAMID
Cairo University, Cairo, Egypt

Received June 6, 1958

Abstract. For applications to orbits with large inclinations the method developed by Brouwer for computing the secula variations of the elements of comets or meteor showers must be extended to include higher powers of $\zeta = \tan i/2$. Thi paper gives the coefficients needed for a development to ζ^6 as well as tables which facilitate the calculation of thes coefficients.

Brouwer (1947) gave a new method for determining the secular perturbations of the elements of a planetary or cometary orbit. A characteristic feature of the method is that it is valid for any elliptic orbit, whatever the value of the eccentricity. However, the following two conditions must be satisfied: (1) the perturbed body must have a direct motion; (2) the aphelion distance of the perturbed orbit must be less than the perihelion distance of the orbit of the perturbing body. The reason for these restrictions is that Brouwer expands the disturbing function in ascending powers of $(\rho/\rho')(1 - \cos i)$, where is the inclination of the perturbed orbit referred to the plane of the orbit of the disturbing body and ρ, ρ' are the heliocentric distances of the disturbed and disturbing bodies, respectively.

Notwithstanding these two limitations the nethod finds many applications in the domain of neteoritic astronomy. With Jupiter as the dominating perturbing planet, there are several showers which have small aphelion distances and lirect orbits. Table I gives a list of some of the orincipal meteoritic showers that satisfy these conditions.

TABLE I. METEORIC SHOWERS WITH DIRECT ORBITS AND APHELION DISTANCES Q LESS THAN JUPITER'S PERIHELION DISTANCE

	i	Q
Night Showers:		
Taurids	13°	4.1 A.U.
Geminids	24	2.6
δ Aquarids	30	4.6
Daylight Showers:		
o Cetids	34	2.5
Arietids	18	2.9
ζ Perseids	4	3.0
β Taurids	6	2.5 to 10.3

The secular perturbations by Jupiter on meteoric orbits are of particular importance in connection with problems concerning the origin and evolution of meteoric streams. Whipple (1940), Brouwer (1947), Plavec (1950) and Whipple and Hamid (1952) have considered these problems in recent years.

In an application of the method to the mean orbit of the Geminids it is necessary, on account of the large inclination, to push the expansion of the disturbing function to higher terms than Brouwer required in the application in his paper. I find that terms up to $(1 - \cos i)^3$ should be included; i.e., terms up to ζ^6 (where $\zeta = \tan i/2$), while Brouwer's expansions includes terms up to ζ^3.

Let h be the longitude of the ascending node, g the argument of the perihelion, and $y = 1 - \cos i$. If the eccentricity of Jupiter's orbit is neglected, the differential equations for the secular perturbations in these elements are:

$$\frac{g}{\tau} = \frac{H}{[(1-y)^2 - H^2]^{\frac{1}{2}}} \{[A_0^0] + y[[A_1^0] + ([A_1^2] + [B_1^2]) \cos 2g] + y^2[[A_2^0] + ([A_2^2] + [B_2^2]) \cos 2g + ([A_2^4] + [B_2^4]) \cos 4g] + y^3[[A_3^0] + ([A_3^2] + [B_3^2]) \cos 2g + ([A_3^4] + [B_3^4]) \cos 4g + ([A_3^6] + [B_3^6]) \cos 6g] + \cdots\}$$

$$+ \frac{(1-y)^2}{H} \{[C_0^0] + [C_0^2] \cos 2g + y[[C_1^0] + [C_1^2] \cos 2g + [C_1^4] \cos 4g] + y^2[[C_2^0] + [C_2^2] \cos 2g + [C_2^4] \cos 4g + [C_2^6] \cos 6g] + y^3[[C_3^0] + [C_3^2] \cos 2g + [C_3^4] \cos 4g + [C_3^6] \cos 6g + [C_3^8] \cos 8g] + \cdots\}$$

$$\frac{y}{\tau} = \frac{(1-y)^2}{H} \{y \cdot [E_1^2] \sin 2g + y^2[[E_2^2] \sin 2g + [E_2^4] \sin 4g] + y^3[[E_3^2] \sin 2g + [E_3^4] \sin 4g + [E_3^6] \sin 6g] + \cdots\}$$

$$\frac{h}{\tau} = -\frac{(1-y)}{H} \{[C_0^0] + [C_0^2] \cos 2g + y[[C_1^0] + [C_1^2] \cos 2g + [C_1^4] \cos 4g] + y^2[[C_2^0] + [C_2^2] \cos 2g + [C_2^4] \cos 4g + [C_2^6] \cos 6g] + y^3[[C_3^0] + [C_3^2] \cos 2g + [C_3^4] \cos 4g + [C_3^6] \cos 6g + [C_3^8] \cos 8g] + \cdots\}$$

In these expressions, if e is the eccentricity of the orbit,

$$H = (1 - e^2)^{\frac{1}{2}} \cos i,$$

and τ is an angular variable related to the time by

$$d\tau = m'k(m_\odot \alpha)^{-\frac{1}{2}}(a')^{-\frac{3}{2}}\, dt$$

where k^2 is the Gaussian constant, a' the semi-major axis, and m' the mass of the disturbing planet, and α the ratio of the semi-major axis of the disturbing body to that of the disturbing planet.

The symbol $[A_k{}^j]$ designates the time average of the term $A_k{}^j$. It is given by

$$[A_k{}^j] = \frac{1}{2\pi}\int_0^{2\pi} A_k{}^j dl,$$

where l is the mean anomaly of the disturbed body. The time average is usually determined by quadrature. Thus $A_k{}^j$ must be computed for different values of l. Similar definitions hold for $[B_k{}^j]$, $[C_k{}^j]$, and $[E_k{}^j]$.

These quantities arise in the development of the disturbed function as follows. Put

$$\Delta^2 = 1 + \rho^2 - 2\rho \cos S,$$

where ρ is the ratio of the heliocentric distance of the perturbed body to the semi-major axis of the disturbing body. The reciprocal of Δ and its

TABLE II. COEFFICIENTS FOR THE CALCULATION OF SECULAR PERTURBATIONS
ARGUMENT: $p = \rho^2/(1 - \rho^2)$

p	$C_0{}^0$	$C_1{}^0$	$C_2{}^0$	$C_3{}^0$	$C_0{}^2/\cos 2v$	$C_1{}^2/\cos 2v$	$C_2{}^2/\cos 2v$	$C_3{}^2/\cos 2v$
.00	+0.00000	−0.00000	+0.00000	−0.00000	−0.00000	+0.00000	−0.00000	+0.00000
.01	0.00757	0.00807	0.00079	0.00032	0.00757	0.00823	0.00105	0.00044
.02	0.01526	0.01730	0.00334	0.00163	0.01526	0.01798	0.00450	0.00228
.03	0.02309	0.02776	0.00799	0.00453	0.02309	0.02931	0.01081	0.00643
.04	0.03105	0.03949	0.01506	0.00974	0.03105	0.04230	0.02048	0.01398
.05	0.03914	0.05254	0.02493	0.01815	0.03914	0.05701	0.03405	0.02629
.06	0.04736	0.06699	0.03800	0.03078	0.04736	0.07353	0.05209	0.04492
.07	0.05571	0.08287	0.05468	0.04885	0.05571	0.09193	0.07522	0.07175
.08	0.06419	0.10026	0.07543	0.07375	0.06419	0.11228	0.10412	0.10893
.09	0.07281	0.11920	0.10073	0.10712	0.07281	0.13467	0.13950	0.15898
.10	0.08155	0.13976	0.13110	0.15081	0.08155	0.15917	0.18210	0.22477
.11	0.09043	0.16200	0.16710	0.20692	0.09043	0.18586	0.23275	0.30958
.12	0.09943	0.18598	0.20929	0.27785	0.09943	0.21483	0.29229	0.41713
.13	0.10857	0.21176	0.25830	0.36629	0.10857	0.24615	0.36165	0.55160
.14	0.11783	0.23940	0.31478	0.47527	0.11783	0.27992	0.44178	0.71774
.15	0.12723	0.26897	0.37942	0.60817	0.12723	0.31622	0.53370	0.92081
.16	0.13676	0.30053	0.45297	0.76875	0.13676	0.35512	0.63850	1.16670
.17	0.14641	0.33415	0.53617	0.96120	0.14641	0.39673	0.75732	1.46198
.18	0.15620	0.36990	0.62986	1.19015	0.15620	0.44113	0.89136	1.81389
.19	0.16612	0.40784	0.73488	1.46071	0.16612	0.48841	1.04188	2.23045
.20	0.17617	0.44804	0.85213	1.77850	0.17617	0.53867	1.21022	2.72049
.21	0.18635	0.49057	0.98255	2.14971	0.18635	0.59198	1.39777	3.29373
.22	0.19665	0.53551	1.12715	2.58110	0.19665	0.64846	1.60601	3.96081
.23	0.20709	0.58292	1.28695	3.08008	0.20709	0.70819	1.83648	4.73337
.24	0.21766	0.63287	1.46305	3.65471	0.21766	0.77127	2.09078	5.62412
.25	0.22836	0.68544	1.65659	4.31379	0.22836	0.83780	2.37062	6.64692
.26	0.23919	0.74070	1.86875	5.06688	0.23919	0.90787	2.67775	7.81684
.27	0.25015	0.79873	2.10079	5.92434	0.25015	0.98159	3.01404	9.15022
.28	0.26123	0.85960	2.35400	6.89740	0.26123	1.05905	3.38141	10.66477
.29	0.27245	0.92339	2.62975	7.99821	0.27245	1.14037	3.78189	12.37968
.30	0.28380	0.99018	2.92944	9.23988	0.28380	1.22564	4.21757	14.31565
.31	0.29528	1.06005	3.25456	10.63654	0.29528	1.31497	4.69065	16.49502
.32	0.30688	1.13307	3.60664	12.20342	0.30688	1.40846	5.20341	18.94184
.33	0.31862	1.20932	3.98728	13.95688	0.31862	1.50623	5.75824	21.68200
.34	0.33049	1.28890	4.39814	15.91451	0.33049	1.60837	6.35761	24.74332
.35	0.34248	1.37187	4.84096	18.09516	0.34248	1.71500	7.00409	28.15563
.36	0.35461	1.45833	5.31753	20.51903	0.35461	1.82624	7.70036	31.95090
.37	0.36687	1.54836	5.82972	23.20775	0.36687	1.94219	8.44920	36.16338
.38	0.37925	1.64203	6.37946	26.18443	0.37925	2.06296	9.25350	40.82966
.39	0.39177	1.73945	6.96877	29.47374	0.39177	2.18867	10.11624	45.98885
.40	0.40441	1.84069	7.59973	33.10202	0.40441	2.31945	11.04053	51.68267
.41	0.41718	1.94584	8.27450	37.09733	0.41718	2.45539	12.02959	57.95560
.42	0.43009	2.05499	8.99532	41.48955	0.43009	2.59663	13.08675	64.85504
.43	0.44312	2.16824	9.76451	46.31048	0.44312	2.74328	14.21549	72.43139
.44	+0.45628	−2.28567	+10.58446	−51.59384	−0.45628	+2.89546	−15.41934	+80.73815

TABLE II (*continued*)

p	$C_1^4/\cos 4v$	$C_2^4/\cos 4v$	$C_3^4/\cos 4v$	$C_2^6/\cos 6v$	$C_3^6/\cos 6v$	$C_3^8/\cos 8v$
.00	−0.00000	+0.00000	−0.00000	−0.00000	+0.00000	−0.00000
.01	0.00017	0.00027	0.00013	0.00000	0.00001	0.00000
.02	0.00068	0.00119	0.00072	0.00003	0.00007	0.00000
.03	0.00156	0.00293	0.00214	0.00010	0.00025	0.00001
.04	0.00281	0.00566	0.00486	0.00024	0.00064	0.00002
.05	0.00447	0.00960	0.00946	0.00048	0.00138	0.00005
.06	0.00654	0.01495	0.01662	0.00086	0.00259	0.00011
.07	0.00905	0.02194	0.02717	0.00139	0.00448	0.00021
.08	0.01202	0.03083	0.04206	0.00213	0.00725	0.00037
.09	0.01547	0.04188	0.06242	0.00311	0.01118	0.00062
.10	0.01940	0.05538	0.08955	0.00438	0.01656	0.00098
.11	0.02386	0.07163	0.12494	0.00597	0.02376	0.00148
.12	0.02885	0.09095	0.17030	0.00795	0.03318	0.00216
.13	0.03440	0.11370	0.22755	0.01035	0.04531	0.00308
.14	0.04052	0.14024	0.29888	0.01324	0.06069	0.00428
.15	0.04725	0.17096	0.38674	0.01668	0.07992	0.00582
.16	0.05459	0.20627	0.49387	0.02073	0.10369	0.00778
.17	0.06258	0.24661	0.62333	0.02546	0.13279	0.01023
.18	0.07123	0.29243	0.77853	0.03093	0.16808	0.01328
.19	0.08057	0.34424	0.96325	0.03723	0.21052	0.01701
.20	0.09062	0.40253	1.18164	0.04443	0.26119	0.02154
.21	0.10141	0.46784	1.43830	0.05262	0.32128	0.02701
.22	0.11295	0.54075	1.73827	0.06189	0.39210	0.03354
.23	0.12527	0.62184	2.08708	0.07232	0.47510	0.04131
.24	0.13840	0.71175	2.49079	0.08402	0.57185	0.05047
.25	0.15236	0.81112	2.95599	0.09710	0.68409	0.06124
.26	0.16717	0.92065	3.48989	0.11165	0,81373	0.07380
.27	0.18286	1.04104	4.10030	0.12779	0.96283	0.08841
.28	0.19946	1.17306	4.79572	0.14565	1.13365	0.10529
.29	0.21698	1.31747	5.58535	0.16533	1.32863	0.12474
.30	0.23546	1.47511	6.47914	0.18699	1.55042	0.14706
.31	0.25492	1.64683	7.48783	0.21074	1.80190	0.17255
.32	0.27539	1.83351	8.62302	0.23674	2.08618	0.20159
.33	0.29690	2.03609	9.89719	0.26512	2.40660	0.23454
.34	0.31947	2.25552	11.32377	0.29605	2.76679	0.27184
.35	0.34313	2.49282	12.91719	0.32969	3.17063	0.31391
.36	0.36791	2.74903	14.69291	0.36619	3.62228	0.36124
.37	0.39383	3.02523	16.66753	0.40575	4.12625	0.41434
.38	0.42093	3.32256	18.85878	0.44853	4.68733	0.47378
.39	0.44923	3.64219	21.28563	0.49472	5.31068	0.54015
.40	0.47876	3.98533	23.96836	0.54453	6.00181	0.61409
.41	0.50955	4.35324	26.92857	0.59815	6.76658	0.69628
.42	0.54164	4.74723	30.18931	0.65580	7.61129	0.78746
.43	0.57504	5.16866	33.77513	0.71768	8.54263	0.88841
.44	−0.60980	+5.61892	−37.71206	−0.78404	+9.56771	−0.99995

odd powers can be expressed by the infinite series

$$\Delta^{-1} = \tfrac{1}{2}b_0 + \sum_1^\infty b_j \cos jS,$$

$$\Delta^{-3} = \tfrac{1}{2}c_0 + \sum_1^\infty c_j \cos jS,$$

$$\Delta^{-5} = \tfrac{1}{2}e_0 + \sum_1^\infty e_j \cos jS,$$

$$\Delta^{-7} = \tfrac{1}{2}f_0 + \sum_1^\infty f_j \cos jS,$$

$$\Delta^{-9} = \tfrac{1}{2}g_0 + \sum_1^\infty g_j \cos jS.$$

The coefficients $b_j \cdots g_j$ are functions of ρ. They can be obtained from the tables by Brown and Brouwer (1932) as functions of $p = \rho^2/(1-\rho^2)$. Let primes denote derivatives of $b_j \cdots g_j$ with respect to ρ. Then, if v is the true anomaly of the disturbed body,

$$2A_0^0 = -b_0'\cdot\alpha\cos v$$

$$4A_1^0 = +(c_1 + \rho c_1')\cdot\alpha\cos v$$

$$32A_2^0 = -3\rho[\rho(2e_0' + e_2') + 2(2e_0 + e_2)]\cdot\alpha\cos v$$

$$128A_3^0 = +5\rho^2[\rho(f_3' + 9f_1') + 3(f_3 + 9f_1)]\cdot\alpha\cos v$$

$$4A_1^2 = -(c_1 + \rho c_1')\cdot\alpha\cos v\cos 2v$$

$$16A_2^2 = +3\rho[\rho(e_0' + e_2') + 2(e_0 + e_2)]\cdot\alpha\cos v\cos 2v$$

$$128A_3^2 = -15\rho^2[\rho(f_3' + 4f_1') + 3(f_3 + 4f_1)]\cdot\alpha\cos v\cos 2v$$

$$32A_2^4 = -3\rho(\rho e_2' + 2e_2)\cdot\alpha\cos v\cos 4v$$

$$128A_3^4 = +15\rho^2[\rho(f_3' + f_1') + 3(f_3 + f_1)]\cdot\alpha\cos v\cos 4v$$

$$128A_3^6 = -5\rho^2(\rho f_3' + 3f_3)\cdot\alpha\cos v\cos 6v$$

$$4C_0^0 = +\rho c_1$$
$$16C_1^0 = +3\rho^2(2e_0 + e_2)$$
$$128C_2^0 = +15\rho^3(f_3 + 9f_1)$$
$$512C_3^0 = -35\rho^4(18g_0 + 16g_2 + g_4)$$

$$4C_0^2 = -\rho c_1\cdot\cos 2v$$
$$8C_1^2 = -3\rho^2(e_0 + e_2)\cos 2v$$
$$128C_2^2 = -45\rho^3(4f_1 + f_3)\cos 2v$$
$$128C_3^2 = +35\rho^4(6g_0 + 7g_2 + g_4)\cos 2v$$

$$16C_1^4 = -3\rho^2 e_2\cos 4v$$
$$128C_2^4 = +45\rho^3(f_1 + f_3)\cos 4v$$
$$256C_3^4 = -35\rho^4(3g_0 + 8g_2 + 3g_4)\cos 4v$$

$$128C_2^6 = -15\rho^3 f_3\cos 6v$$
$$128C_3^6 = +35\rho^4(g_2 + g_4)\cos 6v$$

$$512C_3^8 = -35\rho^4 g_4\cos 8v$$

$$B_1^2 = (2C_0^2/\cos 2v)\cdot\sin 2v\cdot v_e$$
$$B_2^2 = (C_1^2/\cos 2v)\cdot\sin 2v\cdot v_e$$
$$3B_3^2 = (2C_2^2/\cos 2v)\cdot\sin 2v\cdot v_e$$

$$B_2^4 = (2C_1^4/\cos 4v)\cdot\sin 4v\cdot v_e$$
$$3B_3^4 = (4C_2^4/\cos 4v)\cdot\sin 4v\cdot v_e$$

$$B_3^6 = (2C_2^6/\cos 6v)\cdot\sin 6v\cdot v_e$$

$E_1^2 = 2C_0^2$ $E_2^2 = C_1^2$ $3E_3^2 = 2C_2^2$
$E_2^4 = 2C_1^4$ $3E_3^4 = 4C_2^4$
$E_3^6 = 2C_2^6$

The notation v_e has been used for the partial derivative of v with respect to e.

Table II gives with the argument $p = \rho^2/(1 - \rho^2)$ the values of the functions $A_k^j/\alpha\cos v\cos jv$, and $C_k^j/\cos jv$. They depend on ρ only and can therefore be computed once and for all. These same

TABLE II (*continued*)

p	$\frac{A_0^0}{\rho\cdot\alpha\cos v}$	$\frac{A_1^0}{\rho\cdot\alpha\cos v}$	$\frac{A_2^0}{\rho\cdot\alpha\cos v}$	$\frac{A_3^0}{\rho\cdot\alpha\cos v}$	$\frac{A_1^2}{\rho\cdot\alpha\cos v\cos 2v}$	$\frac{A_2^2}{\rho\cdot\alpha\cos v\cos 2v}$	$\frac{A_3^2}{\rho\cdot\alpha\cos v\cos 2v}$	$\frac{A_2^4}{\rho\cdot\alpha\cos v\cos 4v}$	$\frac{A_3^4}{\rho\cdot\alpha\cos v\cos 4v}$	$\frac{A_3^6}{\rho\cdot\alpha\cos v\cos 6v}$
.00	−0.50000	+1.50000	− 0.75000	+ 0.00000	−1.50000	+ 0.75000	− 0.00000	−0.00000	+ 0.00000	−0.00000
.01	0.50563	1.55692	0.88153	0.11022	1.55692	0.91588	0.14815	0.03436	0.03865	0.00072
.02	0.51126	1.61519	1.02331	0.24594	1.61519	1.09521	0.33295	0.07190	0.09004	0.00302
.03	0.51690	1.67483	1.17582	0.41021	1.67483	1.28862	0.55891	0.11280	0.15588	0.00718
.04	0.52254	1.73585	1.33958	0.60633	1.73585	1.49679	0.83089	0.15722	0.23802	0.01347
.05	0.52818	1.79827	1.51509	0.83784	1.79827	1.72041	1.15411	0.20532	0.33845	0.02219
.06	0.53383	1.86210	1.70289	1.10855	1.86210	1.96017	1.53418	0.25728	0.45930	0.03367
.07	0.53949	1.92735	1.90353	1.42252	1.92735	2.21681	1.97714	0.31328	0.60289	0.04827
.08	0.54514	1.99406	2.11756	1.78412	1.99406	2.49107	2.48942	0.37351	0.77166	0.06636
.09	−0.55081	+2.06221	− 2.34555	+ 2.19799	−2.06221	+ 2.78370	− 3.07790	−0.43815	+ 0.96827	−0.08835

p	$\frac{A_0^0}{\alpha\cos v}$	$\frac{A_1^0}{\alpha\cos v}$	$\frac{A_2^0}{\alpha\cos v}$	$\frac{A_3^0}{\alpha\cos v}$	$\frac{A_1^2}{\alpha\cos v\cos 2v}$	$\frac{A_2^2}{\alpha\cos v\cos 2v}$	$\frac{A_3^2}{\alpha\cos v\cos 2v}$	$\frac{A_2^4}{\alpha\cos v\cos 4v}$	$\frac{A_3^4}{\alpha\cos v\cos 4v}$	$\frac{A_3^6}{\alpha\cos v\cos 6v}$
.10	−0.16778	+0.64278	− 0.78034	+ 0.80477	−0.64278	+ 0.93333	− 1.13065	−0.15299	+ 0.36047	−0.03458
.11	0.17696	0.69349	0.89587	1.00823	0.69349	1.07891	1.42082	0.18304	0.45850	0.04591
.12	0.18586	0.74486	1.02104	1.24533	0.74486	1.23724	1.75990	0.21620	0.57424	0.05967
.13	0.19452	0.79699	1.15635	1.51971	0.79699	1.40897	2.15326	0.25262	0.70973	0.07619
.14	0.20297	0.84996	1.30231	1.83525	0.84996	1.59476	2.60665	0.29244	0.86719	0.09579
.15	0.21123	0.90385	1.45943	2.19610	0.90385	1.79526	3.12623	0.33583	1.04899	0.11886
.16	0.21933	0.95872	1.62822	2.60673	0.95872	2.01117	3.71862	0.38295	1.25768	0.14579
.17	0.22728	1.01463	1.80923	3.07190	1.01463	2.24320	4.39087	0.43397	1.49596	0.17700
.18	0.23510	1.07163	2.00302	3.59670	1.07163	2.49209	5.15052	0.48907	1.76677	0.21295
.19	0.24281	1.12976	2.21014	4.18654	1.12976	2.75857	6.00559	0.54842	2.07319	0.25413
.20	0.25040	1.18905	2.43119	4.84717	1.18905	3.04341	6.96465	0.61222	2.41853	0.30105
.21	0.25790	1.24955	2.66675	5.58473	1.24955	3.34741	8.03677	0.68066	2.80631	0.35428
.22	0.26531	1.31129	2.91744	6.40571	1.31129	3.67137	9.23161	0.75393	3.24028	0.41439
.23	0.27264	1.37430	3.18388	7.31702	1.37430	4.01612	10.55941	0.83224	3.72442	0.48203
.24	0.27990	1.43860	3.46672	8.32596	1.43860	4.38253	12.03103	0.91581	4.26283	0.55785
.25	0.28708	1.50423	3.76661	9.44025	1.50423	4.77145	13.65796	1.00483	4.86028	0.64257
.26	0.29421	1.57120	4.08424	10.66808	1.57120	5.18378	15.45235	1.09955	5.52121	0.73694
.27	0.30127	1.63955	4.42028	12.01809	1.63955	5.62045	17.42705	1.20017	6.25072	0.84176
.28	0.30828	1.70930	4.77545	13.49939	1.70930	6.08238	19.59561	1.30693	7.05409	0.95786
.29	0.31524	1.78046	5.15047	15.12159	1.78046	6.57055	21.97235	1.42008	7.93690	1.08614
.30	0.32215	1.85307	5.54608	16.89484	1.85307	7.08592	24.57234	1.53985	8.90503	1.22753
.31	0.32901	1.92715	5.96304	18.82980	1.92715	7.62952	27.41145	1.66649	9.96469	1.38303
.32	0.33584	2.00270	6.40212	20.93769	2.00270	8.20238	30.50639	1.80026	11.12240	1.55369
.33	0.34262	2.07976	6.86412	23.23030	2.07976	8.80553	33.87474	1.94141	12.38505	1.74061
.34	0.34937	2.15835	7.34983	25.72005	2.15835	9.44006	37.53497	2.09022	13.75986	1.94494
.35	0.35609	2.23848	7.86011	28.41996	2.23848	10.10707	41.50646	2.24696	15.25441	2.16791
.36	0.36277	2.32016	8.39579	31.34366	2.32016	10.80769	45.80954	2.41190	16.87667	2.41079
.37	0.36943	2.40343	8.95771	34.50548	2.40343	11.54305	50.46557	2.58533	18.63503	2.67495
.38	0.37605	2.48830	9.54679	37.92046	2.48830	12.31434	55.49692	2.76755	20.53824	2.96178
.39	0.38265	2.57479	10.16391	41.60427	2.57479	13.12274	60.92699	2.95884	22.59549	3.27278
.40	0.38922	2.66291	10.80999	45.57337	2.66291	13.96950	66.78030	3.15951	24.81641	3.60949
.41	0.39577	2.75268	11.48597	49.84496	2.75268	14.85584	73.08250	3.36987	27.21107	3.97353
.42	0.40229	2.84413	12.19279	54.43703	2.84413	15.78304	79.86042	3.59025	29.79002	4.36663
.43	0.40880	2.93726	12.93147	59.36838	2.93726	16.75242	87.14209	3.82095	32.56427	4.79055
.44	−0.41528	+3.03210	−13.70297	+64.65855	−3.03210	+17.76528	−94.95667	−4.06231	+35.54528	−5.24716

unctions may be used for the calculation of B_k^j nd C_k^j since

$$kB_k^j/(j \sin jv \cdot v_e) = C_k^j/\cos jv,$$
$$kE_k^j = jC_k^j.$$

The use of these tables facilitates the compuation of the coefficients necessary for obtaining he differential equations for the secular variaions of the orbital elements. It has been found hat an experienced computer with an electric esk calculator requires about 16 hours for the alculation of the various coefficients in the differntial equations.

The tables were constructed during the author's tudies on the Geminid Shower. This is the eason for restricting the tables to the range $< p < 0.44$. A larger range of values of p will e needed if the tables are to be used for the δ Aquarids and the Taurids. It is my intention to present the results of my study of the Geminids and an extension of the tables in further papers.

I am indebted to Dr. Brouwer for his constructive suggestions and would also like to express my gratitude to Dr. Whipple for his encouragement and help.

REFERENCES

Brouwer, D. 1947, *A. J.* **52**, 190.
Brown, E. W. and Brouwer, D. 1932, *Trans. Yale Obs.* **6**; *Tables for the Development of the Disturbing Functions* (Cambridge Univ. Press).
Ponsen, J. *Leiden Ann.* **20**, 400.
Plavec, M. 1950, *Nature*, **165**, 162.
Whipple, F. L. 1940, *Proc. Amer. Phil. Soc.* **83**, 711; *Harv. Repr.* No. 210.
——. 1956, *Between the Planets* (Harvard Univ. Press: Cambridge), pp. 99, 120.
—— and Hamid, S. 1952, *Bull. Obs. Helwan* No. 41; *Harv. Repr.* No. 361.

PERIODS FOR FORTY-ONE VARIABLE STARS IN SAGITTARIUS

By DORRIT HOFFLEIT
Maria Mitchell Observatory, Nantucket, Massachusetts

Received February 10, 1959

Abstract. Periods have been determined for 15 previously known and 26 new variable stars in Sagittarius. WW Sgr, eretofore believed to be of the U Geminorum type, is found to be a normal long-period variable with a period of 208.5 ays.

Work on Variable Star Field 193 in Sagittarius, egun many years ago at Harvard College Obervatory (Shapley and Swope 1934; Hoffleit 957, 1958), has been actively resumed at the laria Mitchell Observatory. New periods for 1 variable stars are presented herewith: 15 for tars previously listed in the *General Catalogue f Variable Stars* and 26 for hitherto unannounced ariables.

For the majority of the stars the results given Table I are based upon more than 250 photoraphs taken at the southern stations of Harvard bservatory since 1924 and on plates obtained t Nantucket during the past two summers. All f the stars are in the constellation Sagittarius. he first column of the table gives either the ecognized variable-star designation under that onstellation in the 1958 edition of the *General atalogue of Variable Stars*, or a serial number r the variable stars newly announced here. he columns headed J.D. and Ep. give the last ve digits of the Julian date of a well-defined aximum and the number of epochs between the rst and last observations.

The first variable listed in Table I is a Cepheid with a period of nearly 13 days. If it were unobscured its apparent magnitude would indicate a distance considerably beyond the galactic nucleus. The light curve suggests that the star is a Population I object. Determination of its spectrum and reddening would be of considerable interest. Variable No. 3 has a close 12.5 mag. companion which could be clearly resolved only on plates taken with the 24-inch Bruce refractor (scale 1′ = 1 mm). It is probably V1591 Sgr although the observations do not fit the 365-day period given by Ponsen (1955). Variable No. 7, with fairly regular cycles of about 80 to 83 days, appears to belong to the RV Tauri class. All of the other stars listed are Mira-type with periods ranging from 141 to 545 days, all but three being shorter than 350 days.

For two of the stars, LP and MW Sgr, periods had already been published by Innes (1917) but the periods did not satisfy the present observations. Both the new and the older published observations are satisfactorily represented by the revised periods. Another star, WW Sgr, had

TABLE I. NEW PERIODS FOR VARIABLE STARS IN SAGITTARIUS

Var. Sgr	R.A. (1900)	Dec.	Max. pg	Min. pg	Period	J.D.	Ep.	Obs.	C
	h m s	° ′			d				
1	18 07 19	−26 25·2	12·6	14·9	12·985	24402	964	K, A, Fo	K
2	10 02	−27 24·9	14·3	[16·1	234:	27240	50	K	K
3*	12 39	−27 46·6	12·4	[16·3	193	28340	15	A, K	K
4	13 11	−24 08·5	13·7	[16·3	443	25450	24	A	H
5	14 09	−24 00·5	13·7	[16·3	252:	31600	35	A	H
6	15 42	−27 28·1	12·9	16·2	201·5	27160	49	F	F
7	16 22	−27 37·4	12·1	14·0	80–83	26135		K	K
WW	16 49	−27 28·4	12·2	[16·5	208·5	31600	62	A, K	K
8	17 06	−24 40·2	13·3	15·1	277	24370	36	A, P	C
9	17 36	−27 32·0	12·7	[16·4	237·5	26210	50	A, F	F
10	17 58	−27 42·4	13·8	[16·4	305	36050	39	F	F
GY	19 23	−27 28·1	13·0	[16·5	215	30240	38	A, K	H
LP	21 44	−27 43·9	13·8	[16·	222	27280	42	H	H
11	22 52	−27 06·1	14·0	[16·3	230	25850	43	F	F
HV	23 28	−26 30·5	13·7	[16·0	286	27610	44	Fr	Fr
12	24 39	−26 53·7	13·6	[16·3	325·3	33850	38	F	F
13	24 58	−26 56·5	13·8	[16·3	258	25390	38	F	F
14	24 58	−27 11·4	13·6	[16·3	189	26210	52	F	F
15	25 19	−27 01·8	13·1	[16·3	288:	27270	43	F	F
16	26 02	−26 33·6	12·3	16·1	142·6	26160	85	F	F
IN	26 04	−27 51·4	12·2	[16·2	210	27220	50	A	H
17	26 16	−24 53·8	13·7	[16·	248·5	27260	35	F	F
LS	26 25	−25 34·9	13·7	[16·	214·5	25830	60	A, Fr	Fr
IO	26 41	−25 12·5	12·5	[15·5	210	29050	40	A	H
LT	26 40	−25 22·3	12·3	[15·6	262	29740	32	A, Fo	H
IS	27 39	−25 13·6	13·4	[16·0	493	25440	25	Fr	Fr
18	27 49	−20 17·4	13·6	16·3	271	26200	36	A	H
LU	27 51	−25 37·9	12·8	[16·0	315	33010	26	A	H
19	28 42	−27 06·0	12·8	[16·3	200·3	27300	61	F	F
20	28 56	−26 45·4	13·2	[16·3	261·5	25830	46	F, Fo	F
21	31 31	−20 16·8	13·7	15·8	141	25420	70	A	H
KL	31 57	−23 59·2	13·2	[16·5	236	29430	33	A	H
22	33 05	−25 22·3	13·8	16·4	346	25390	28	A	H
23	33 30	−25 07·7	14·6	[16·2	545	26110	18	A	H
MP	34 26	−26 20·5	13·1	[16·0	149	26500	85	A, M	H
24	35 18	−24 04·0	13·5	[16·2	308	26095	39	F	F
25	36 22	−25 22·2	13·0	16·3	289:	26210	35	A	H
KV	38 25	−23 25·5	12·6	[15·6	230	32380	35	A	H
MW	38 42	−27 44·8	14·0	[16·0	208·5	24400	58	H	H
MX	38 47	−23 38·9	13·8	16·3	228	25400	60	M	M
26	39 50	−25 24·5	13·1	16·2	169	27250	54	F	F

heretofore been listed as a member of the U Geminorum class. This type is not borne out by the observations on Harvard and Nantucket plates. Instead, the older observations (Himpel 1943) as well as our recent data fit a normal long period of 208.5 days.

The work presented here has been carried out mainly during the past two years. From June 1957 to July 1958 it was supported by a grant from the National Science Foundation, and during the summer of 1958 partly by an anonymous gift, partly by a grant from the Gould Fund of the National Academy of Sciences. The students and assistants who participated in the observations and reductions are indicated in the last two columns of the table; the final column denotes the computer of the period of light variation: Jean Hales Andersen (A), Marjorie Crouch (C Choko Fujita (F), Margaret Fothergill (Fo Margo Friedel (Fr), Andrea Kundsin (K), Jane Marshall (M), Zora Prochazka (P), and myse (H). I am indebted to the Director of Harvar College Observatory for the loan of plates fro the Harvard collection and for his permittin Mrs. Andersen to work in the Harvard pla stacks examining some of our brighter variab stars on various series of patrol plates.

REFERENCES

Himpel, K. 1943, *Beob. Zirk.* **No. 25,** 105.
Hoffleit, D. 1957, *A. J.* **62,** 120.
——. 1958, *A. J.* **63,** 28.
Innes, R. T. A. 1917, *Union Obs. Circ.* **No. 37.**
Ponsen, J. *Leiden Ann.* **20,** 400.
Shapley, H. and Swope, H. H. 1934, *Ann. Harv. Coll. O*
90, 188.

STANDARD LIGHT–TIME CURVES

By JOHN B. IRWIN
Goethe Link Observatory, Bloomington, Indiana

Received September 16, 1958

Abstract. The apparent variation of period of an eclipsing binary arising from the variation of distance (changing ght-time) from the observer, as the result of orbital motion with respect to a third component, produces a characteristic rve whose shape depends only on e and ω. Coordinates for a complete set of standard light-time curves are given that ould prove useful in a preliminary analysis of variation of period. Analytical expressions for the least-squares coefficients e given.

The analysis of the variation of period of an clipsing binary can sometimes yield fundamental ata concerning both the eclipsing pair and other ore distant components. For any given system ere may be more than one factor causing a ariation of period and such variations may erefore be complex. One cause for an observed ariation of period may be the orbital motion the eclipsing pair with respect to a distant ird component; the changing distance from a ane perpendicular to the line of sight produces changing light-time. The solution of such a ght-time orbit was first considered by Woltjer 922). Woltjer's method was modified by Irwin 952) who also gave a numerical-graphical ethod of solution. A set of standard light-time rves would appear to be useful in any such alysis and the purpose of this paper is to pro-de tables of coordinates whereby such a set ay be quickly constructed. This set of tables as its counterpart in, and is similar in applica-on to, King's (1920) standard velocity-curves hich are useful in the preliminary analysis of ectroscopic-binary orbits. The computations r the light-time curves are, however, consid-ably lengthier.

The notation here used is the same as in the win (1952) paper. The reference plane, perpen-cular to the line of sight, passes through the nter of the elliptical orbit of the eclipsing pair bout the center of mass of all three stars. The ght time, τ, is taken in the sense of observed me minus computed time, where the computed me is

$$t = t_0 + EP'. \tag{1}$$

can be shown that:

$$= K \frac{1}{\sqrt{1 - e^2\cos^2\omega}} \times \left\{ \frac{1 - e^2}{1 + e\cos v}\sin(v + \omega) + e\sin\omega \right\}, \tag{2}$$

here

$$= \tfrac{1}{2}(\tau_{\max} - \tau_{\min}) = \frac{a\sin i\sqrt{1 - e^2\cos^2\omega}}{2.590 \times 10^{10}}. \tag{3}$$

τ and K are in days and a, the semi-major axis, is in kilometers; the denominator is the velocity of light in km/days. The dimensionless expression

$$\frac{\tau}{K}\frac{1}{\sqrt{1 - e^2\cos^2\omega}} \times \left\{ \frac{1 - e^2}{1 + e\cos v}\sin(v + \omega) + e\sin\omega \right\}$$

varies between ± 1 and is what we are concerned with here; it is tabulated with argument M, the mean anomaly, in Table I for nine values of the eccentricity and ten values of ω. It may be useful in deriving the time of periastron passage (T) to know the mean anomaly (M) at $\tau_{\max}$ and $\tau_{\min}$. Such values of $M = (360°/P)(t - T)$ are given in Table II. At these times the motion of the eclipsing pair is at right angles to the line of sight and, as is well known from spectroscopic-binary theory, $dz/dt = 0$ and $\cos(v + \omega) = -e\cos\omega$.

A sample set of light-time curves for $\omega = 40°$ and for five values of the eccentricity is shown in Figure 1. Because the distortions from a sine curve are, on the average, only half of those encountered in a standard velocity-curve, it probably suffices to plot only five values of the eccentricity—as shown—and for only five values of ω (such as 0°, 20°, 40°, 60° and 80°). This reduces the work of plotting the complete tables by a factor of 4. The tables will be useful for intermediate cases. The observations to be analyzed should be plotted on a separate sheet of transparent or semi-transparent cross-section paper with appropriate horizontal and vertical scales. The best fit is made to the standard curves by trial and error and it should be possible to interpolate in both e and ω. Given e and ω, $a\sin i$ is derived from (3) and T can be determined with the aid of Table II. Representation of the elements and calculation of an ephemeris is accomplished with the aid of (2). The Allegheny Tables, Schlesinger and Udick (1912), will be found useful in deriving the values of v, the true anomaly.

In order to match the observations it may be necessary, if ω lies between 90° and 360°, to invert or reverse the observational plot. If inver-

TABLE I. STANDARD LIGHT-TIME COORDINATES

$e = .10$

M \ ω	0°	10°	20°	30°	40°	50°	60°	70°	80°	90°
0°	0.000	+0.174	+0.344	+0.502	+0.645	+0.768	+0.867	+0.940	+0.985	+1.000
5	+ .097	.269	.433	.583	.716	.826	.911	.969	.997	.995
10	.193	.361	.518	.659	.780	.877	.947	.988	1.000	.981
15	.286	.449	.598	.729	.837	.919	.973	.998	.993	.958
20	.377	.533	.672	.791	.885	.953	.991	.999	.977	.926
30	.547	.684	.801	.893	.958	.993	.998	.973	.919	.837
40	.694	.809	.899	.962	.995	.997	.970	.913	.829	.720
50	.816	.904	.965	.996	.996	.967	.908	.821	.710	.578
60	.908	.967	.997	.996	.964	.904	.816	.703	.570	.419
70	.968	.997	.995	.963	.901	.812	.699	.564	.413	.250
80	.997	.995	.962	.900	.810	.696	.562	.410	.246	+ .075
90	.995	.962	.900	.811	.697	.561	.409	.245	+ 0.74	− .099
100	.964	.902	.813	.699	.564	.412	.248	+ .076	− .097	− .268
110	.905	.817	.704	.569	.417	.253	+ .082	− .092	− .263	− .426
120	.822	.710	.576	.425	.261	+ .090	− .084	− .256	− .419	− .569
130	.718	.585	.435	.272	+ .100	− .074	− .246	− .410	− .562	− .696
140	.596	.447	.284	+ .112	− .062	− .235	− .399	− .552	− .688	− .803
150	.460	.298	+ .127	− .048	− .221	− .387	− .541	− .678	− .795	− .888
160	.313	+ .142	− .033	− .206	− .373	− .529	− .668	− .787	− .882	− .950
170	+ .158	− .017	− .191	− .359	− .516	− .657	− .777	− .875	− .945	− .987
180	.000	− .174	− .344	− .502	− .645	− .768	− .867	− .940	− .985	−1.000
190	− .158	− .328	− .488	− .632	− .757	− .859	− .935	− .982	−1.000	− .987
200	− .313	− .474	− .620	− .747	− .851	− .929	− .979	−1.000	− .990	− .950
210	− .460	− .608	− .737	− .843	− .924	− .976	− .999	− .992	− .954	− .888
220	− .596	− .727	− .836	− .918	− .973	− .998	− .993	− .958	− .894	− .803
230	− .718	− .828	− .913	− .970	− .998	− .994	− .961	− .899	− .810	− .696
240	− .822	− .909	− .968	− .997	− .996	− .964	− .903	− .815	− .703	− .569
250	− .905	− .965	− .996	− .996	− .966	− .907	− .820	− .708	− .575	− .426
260	− .964	− .995	− .997	− .968	− .909	− .823	− .712	− .580	− .430	− .268
270	− .995	− .997	− .969	− .911	− .825	− .714	− .582	− .432	− .270	− .099
280	− .997	− .969	− .911	− .825	− .714	− .582	− .432	− .269	− .099	+ .075
290	− .968	− .910	− .824	− .712	− .579	− .429	− .266	− .095	+ .078	.250
300	− .908	− .821	− .709	− .575	− .424	− .260	− .089	+ .085	.256	.419
310	− .816	− .702	− .567	− .416	− .251	− .079	+ .095	.266	.429	.578
320	− .694	− .558	− .405	− .239	− .067	+ .107	.278	.440	.589	.720
330	− .547	− .392	− .226	− .052	+ .122	.292	.454	.601	.730	.837
340	− .377	− .210	− .036	+ .139	.309	.469	.615	.742	.847	.926
345	− .286	− .115	+ .060	.233	.399	.552	.688	.803	.894	.958
350	− .193	− .018	.156	.326	.485	.630	.755	.857	.933	.981
355	− .097	+ .078	.251	.416	.568	.702	.815	.903	.964	.995
360	0.000	+0.174	+0.344	+0.502	+0.645	+0.768	+0.867	+0.940	+0.985	+1.000

$e = .20$

M \ ω	0°	10°	20°	30°	40°	50°	60°	70°	80°	90°
0°	0.000	+0.177	+0.348	+0.508	+0.650	+0.772	+0.870	+0.942	+0.985	+1.000
5	+ .109	.283	.448	.598	.729	.837	.919	.973	.998	.994
10	.216	.386	.543	.682	.799	.891	.956	.992	.999	.970
15	.320	.483	.630	.757	.859	.935	.982	1.000	.988	.947
20	.420	.574	.709	.822	.909	.968	.997	.996	.966	.908
30	.600	.732	.841	.923	.976	.999	.992	.955	.890	.800
40	.750	.855	.933	.982	1.000	.987	.945	.875	.779	.661
50	.865	.940	.986	1.000	.983	.937	.862	.763	.641	.501
60	.945	.988	1.000	.980	.931	.854	.751	.627	.484	.328
70	.989	1.000	.979	.928	.849	.744	.618	.474	.317	+ .151
80	1.000	.979	.928	.848	.743	.615	.470	.312	+ .145	− .025
90	.981	.931	.852	.746	.618	.472	.313	+ .146	− .025	− .195
100	.935	.858	.754	.626	.480	.321	+ .153	− .019	− .189	− .354
110	.867	.765	.639	.493	.334	.165	− .008	− .179	− .344	− .499
120	.778	.654	.511	.351	.182	+ .009	− .164	− .330	− .487	− .628
130	.673	.531	.373	.204	+ .030	− .144	− .313	− .471	− .614	− .740
140	.554	.398	.230	+ .055	− .121	− .291	− .452	− .598	− .726	− .832
150	.425	.258	+ .083	− .094	− .266	− .430	− .579	− .710	− .820	− .905
160	.287	+ .113	− .064	− .239	− .405	− .557	− .692	− .806	− .895	− .955
170	+ .145	− .033	− .209	− .377	− .533	− .672	− .790	− .883	− .950	− .983
180	.000	− .177	− .348	− .508	− .650	− .772	− .870	− .942	− .985	−1.000
190	− .145	− .318	− .480	− .627	− .754	− .856	− .933	− .981	−1.000	− .98
200	− .287	− .453	− .603	− .734	− .841	− .922	− .975	− .999	− .993	− .958
210	− .425	− .578	− .713	− .826	− .911	− .969	− .997	− .995	− .964	− .905
220	− .554	− .693	− .809	− .900	− .962	− .995	− .997	− .970	− .915	− .832
230	− .673	− .793	− .888	− .955	− .992	− .999	− .975	− .923	− .844	− .740
240	− .778	− .877	− .948	− .989	−1.000	− .979	− .930	− .853	− .751	− .628
250	− .867	− .941	− .986	−1.000	− .983	− .936	− .861	− .761	− .639	− .499
260	− .935	− .983	−1.000	− .985	− .941	− .867	− .768	− .647	− .508	− .354
270	− .981	−1.000	− .987	− .944	− .872	− .773	− .653	− .513	− .359	− .195
280	−1.000	− .988	− .946	− .874	− .776	− .655	− .514	− .360	− .195	− .025
290	− .989	− .946	− .874	− .775	− .653	− .511	− .356	− .190	− .020	+ .151
300	− .945	− .871	− .771	− .647	− .504	− .346	− .179	− .008	+ .163	.328
310	− .865	− .763	− .637	− .491	− .331	− .162	+ .010	+ .181	.347	.501
320	− .750	− .621	− .473	− .310	− .140	+ .035	.206	.371	.524	.661
330	− .600	− .449	− .284	− .111	+ .065	.237	.401	.552	.686	.800
340	− .420	− .252	− .077	+ .099	.272	.435	.584	.714	.823	.908
345	− .320	− .147	+ .030	.205	.373	.529	.667	.785	.879	.947
350	− .216	− .040	.137	.310	.471	.617	.743	.847	.925	.976
355	− .109	+ .069	.244	.411	.564	.699	.812	.900	.961	.994
360	0.000	+0.177	+0.348	+0.508	+0.650	+0.772	+0.870	+0.942	+0.985	+1.000

TABLE I (*continued*)

$e = .30$

ω	0°	10°	20°	30°	40°	50°	60°	70°	80°	90°
0°	0.000	+0.182	+0.356	+0.518	+0.660	+0.781	+0.876	+0.945	+0.986	+1.000
5	+.124	.302	.470	.620	.749	.852	.929	.978	.999	.992
0	.246	.418	.575	.712	.825	.910	.968	.996	.997	.969
5	.362	.525	.670	.792	.887	.954	.991	.999	.979	.932
0	.471	.623	.755	.860	.936	.983	1.000	.988	.948	.882
0	.661	.786	.885	.954	.992	.999	.976	.926	.850	.751
0	.808	.902	.965	.996	.996	.965	.906	.822	.715	.589
0	.911	.971	.998	.993	.956	.891	.801	.688	.558	.412
0	.973	.999	.991	.952	.882	.787	.671	.536	.388	.230
0	.999	.991	.951	.880	.783	.663	.525	.374	.214	+.049
0	.992	.954	.883	.785	.664	.524	.371	.209	+.043	−.123
0	.959	.891	.795	.673	.533	.378	.214	+.047	−.121	−.284
0	.903	.809	.690	.549	.393	.228	+.058	−.111	−.275	−.431
0	.827	.711	.572	.416	.249	+.078	−.094	−.260	−.417	−.562
0	.736	.600	.446	.278	+.105	−.069	−.239	−.399	−.546	−.678
0	.631	.480	.313	+.139	−.038	−.211	−.375	−.525	−.660	−.775
0	.517	.352	.178	−.001	−.177	−.346	−.501	−.639	−.759	−.856
0	.394	.221	+.041	−.138	−.311	−.471	−.615	−.739	−.841	−.919
0	.266	+.086	−.095	−.272	−.437	−.586	−.716	−.823	−.907	−.964
0	+.134	−.048	−.228	−.399	−.554	−.690	−.803	−.892	−.955	−.991
0	.000	−.182	−.356	−.518	−.660	−.781	−.876	−.945	−.986	−1.000
0	−.134	−.312	−.478	−.628	−.755	−.857	−.933	−.980	−.999	−.991
0	−.266	−.437	−.592	−.727	−.836	−.919	−.973	−.998	−.995	−.964
0	−.394	−.555	−.696	−.813	−.903	−.964	−.995	−.997	−.972	−.919
0	−.517	−.664	−.788	−.885	−.953	−.991	−.999	−.978	−.930	−.856
0	−.631	−.762	−.866	−.942	−.986	−1.000	−.984	−.940	−.869	−.775
0	−.736	−.846	−.929	−.980	−1.000	−.989	−.948	−.881	−.790	−.678
0	−.827	−.915	−.973	−.999	−.992	−.956	−.891	−.802	−.692	−.562
0	−.903	−.966	−.997	−.995	−.962	−.900	−.813	−.703	−.574	−.431
0	−.959	−.995	−.997	−.967	−.907	−.821	−.711	−.583	−.439	−.284
0	−.992	−.998	−.971	−.913	−.826	−.716	−.586	−.442	−.286	−.123
0	−.999	−.973	−.916	−.829	−.717	−.586	−.439	−.281	−.117	+.049
0	−.973	−.915	−.828	−.714	−.579	−.429	−.268	−.102	+.065	.230
0	−.911	−.821	−.704	−.566	−.412	−.248	−.079	+.090	.255	.412
0	−.808	−.687	−.545	−.386	−.217	−.045	+.127	.292	.447	.589
0	−.661	−.513	−.350	−.177	.000	+.173	.339	.492	.631	.751
0	−.471	−.303	−.126	+.054	+.229	.394	.545	.679	.792	.882
5	−.362	−.186	−.006	.173	.344	.502	.642	.762	.859	.932
0	−.246	−.065	+.116	.292	.456	.603	.731	.835	.915	.969
5	−.124	+.058	.238	.408	.562	.697	.809	.897	.958	.992
0	0.000	+0.182	+0.356	+0.518	+0.660	+0.781	+0.876	+0.945	+0.986	+1.000

$e = .40$

ω	0°	10°	20°	30°	40°	50°	60°	70°	80°	90°
0°	0.000	+0.189	+0.369	+0.533	+0.675	+0.793	+0.884	+0.949	+0.987	+1.000
5	+.145	.329	.500	.650	.775	.873	.942	.984	1.000	.989
0	.284	.460	.618	.752	.857	.933	.980	.999	.992	.959
5	.415	.579	.721	.836	.920	.974	.998	.994	.964	.910
0	.533	.683	.808	.902	.965	.996	.997	.971	.920	.846
0	.727	.844	.929	.981	1.000	.987	.947	.881	.793	.686
0	.864	.944	.989	.999	.977	.926	.849	.751	.634	.503
0	.950	.992	.998	.970	.912	.827	.721	.597	.460	.313
0	.992	.998	.969	.907	.817	.705	.576	.434	.283	+.126
0	.999	.971	.910	.818	.703	.569	.423	.268	+.110	−.050
0	.977	.919	.829	.712	.576	.425	.267	+.106	−.056	−.215
0	.931	.846	.731	.594	.441	.279	+.114	−.051	−.211	−.364
0	.867	.757	.622	.468	.303	+.134	−.035	−.198	−.353	−.498
0	.787	.657	.504	.338	.165	−.009	−.176	−.335	−.483	−.616
0	.695	.547	.381	.205	+.028	−.146	−.310	−.462	−.599	−.719
0	.593	.431	.254	+.073	−.106	−.276	−.434	−.576	−.700	−.805
0	.483	.309	+.126	−.057	−.234	−.399	−.548	−.677	−.787	−.875
0	.368	.185	−.001	−.185	−.357	−.513	−.650	−.766	−.859	−.930
0	.248	+.060	−.128	−.307	−.472	−.617	−.741	−.841	−.917	−.969
0	+.124	−.065	−.251	−.424	−.578	−.711	−.819	−.902	−.960	−.992
0	.000	−.189	−.369	−.533	−.675	−.793	−.884	−.949	−.987	−1.000
0	−.124	−.310	−.482	−.634	−.762	−.862	−.935	−.981	−.999	−.992
0	−.248	−.426	−.588	−.726	−.837	−.919	−.972	−.997	−.996	−.969
0	−.368	−.537	−.685	−.807	−.899	−.961	−.994	−.999	−.977	−.930
0	−.483	−.640	−.772	−.876	−.948	−.989	−1.000	−.983	−.941	−.875
0	−.593	−.735	−.849	−.931	−.981	−1.000	−.989	−.951	−.889	−.805
0	−.695	−.819	−.912	−.971	−.998	−.994	−.960	−.902	−.820	−.719
0	−.787	−.890	−.959	−.995	−.997	−.969	−.913	−.834	−.734	−.616
0	−.867	−.946	−.990	−.999	−.976	−.923	−.846	−.747	−.630	−.498
0	−.931	−.983	−1.000	−.982	−.933	−.856	−.757	−.640	−.508	−.364
0	−.977	−1.000	−.987	−.941	−.865	−.765	−.646	−.513	−.368	−.215
0	−.999	−.990	−.947	−.872	−.771	−.649	−.512	−.364	−.209	−.050
0	−.992	−.950	−.875	−.772	−.646	−.505	−.352	−.194	−.034	+.126
0	−.950	−.874	−.767	−.637	−.489	−.331	−.168	−.004	+.157	.313
0	−.864	−.754	−.618	−.463	−.298	−.128	+.040	+.204	.359	.503
0	−.727	−.585	−.423	−.250	−.073	+.100	.266	.421	.561	.686
0	−.533	−.364	−.183	.000	+.178	.346	.498	.634	.750	.846
5	−.415	−.235	−.050	+.134	.308	.468	.610	.732	.832	.910
0	−.284	−.098	+.090	.270	.438	.587	.714	.820	.901	.959
5	−.145	+.045	.231	.405	.562	.696	.807	.893	.954	.989
0.	0.000	+0.189	+0.369	+0.533	+0.675	+0.793	+0.884	+0.949	+0.987	+1.000

TABLE I (*continued*)

$e = .50$

M \ ω	0°	10°	20°	30°	40°	50°	60°	70°	80°	90°
0°	0.000	+0.200	+0.387	+0.555	+0.696	+0.809	+0.894	+0.954	+0.989	+1.00
5	+ .173	.366	.541	.690	.809	.898	.958	.991	1.000	[illegible]
10	.336	.517	.674	.802	.897	.959	.993	.999	.982	[illegible]
15	.482	.647	.784	.887	.956	.992	.999	.981	.939	[illegible]
20	.606	.754	.868	.946	.989	1.000	.982	.940	.877	[illegible]
30	.797	.901	.969	.998	.993	.957	.897	.816	.718	[illegible]
40	.915	.977	1.000	.985	.938	.864	.770	.660	.537	[illegible]
50	.978	1.000	.982	.929	.847	.743	.623	.492	.353	[illegible]
60	1.000	.984	.931	.845	.734	.607	.468	.323	.174	[illegible]
70	.989	.941	.856	.743	.610	.464	.313	.159	+ .006	[illegible]
80	.955	.876	.765	.629	.478	.320	.160	+ .003	− .151	[illegible]
90	.900	.795	.661	.508	.344	.177	+ .013	− .144	− .294	[illegible]
100	.832	.703	.550	.383	.210	+ .038	− .126	− .281	− .425	[illegible]
110	.749	.602	.434	.256	+ .077	− .095	− .257	− .406	− .541	[illegible]
120	.658	.495	.315	.130	− .051	− .222	− .379	− .520	− .645	[illegible]
130	.559	.382	.194	+ .005	− .176	− .342	− .492	− .623	− .735	[illegible]
140	.454	.267	+ .073	− .117	− .294	− .454	− .594	− .713	− .812	[illegible]
150	.344	.150	− .046	− .234	− .406	− .557	− .686	− .792	− .876	[illegible]
160	.231	+ .032	− .164	− .347	− .511	− .651	− .767	− .858	− .927	[illegible]
170	+ .116	− .084	− .278	− .454	− .608	− .735	− .836	− .912	− .964	[illegible]
180	.000	− .200	− .387	− .555	− .696	− .809	− .894	− .954	− .989	−1.00
190	− .116	− .312	− .492	− .648	− .775	− .872	− .940	− .982	− .999	[illegible]
200	− .231	− .421	− .590	− .732	− .843	− .923	− .974	− .997	− .997	[illegible]
210	− .344	− .525	− .681	− .807	− .901	− .962	− .994	− .999	− .980	[illegible]
220	− .454	− .623	− .764	− .872	− .946	− .988	−1.000	− .986	− .949	[illegible]
230	− .559	− .713	− .837	− .925	− .978	− .999	− .992	− .959	− .904	[illegible]
240	− .658	− .795	− .898	− .965	− .997	− .996	− .968	− .916	− .844	[illegible]
250	− .749	− .866	− .947	− .991	− .999	− .976	− .927	− .857	− .768	[illegible]
260	− .832	− .925	− .982	−1.000	− .984	− .939	− .869	− .780	− .675	[illegible]
270	− .900	− .969	− .999	− .991	− .949	− .881	− .792	− .686	− .566	[illegible]
280	− .955	− .995	− .995	− .960	− .893	− .802	− .693	− .571	− .439	[illegible]
290	− .989	− .998	− .968	− .904	− .812	− .699	− .572	− .436	− .293	[illegible]
300	−1.000	− .975	− .912	− .819	− .702	− .569	− .426	− .278	− .128	[illegible]
310	− .978	− .917	− .821	− .699	− .558	− .407	− .252	− .096	+ .057	[illegible]
320	− .915	− .816	− .687	− .538	− .377	− .212	− .049	+ .110	.261	[illegible]
330	− .797	− .660	− .500	− .328	− .152	+ .020	+ .184	.337	.477	[illegible]
340	− .606	− .437	− .252	− .065	+ .117	.286	.439	.575	.694	[illegible]
345	− .482	− .297	− .105	+ .085	.264	.426	.568	.691	.794	[illegible]
350	− .336	− .141	+ .055	.243	.414	.565	.692	.797	.880	[illegible]
355	− .173	+ .027	.222	.403	.561	.695	.804	.887	.948	[illegible]
360	0.000	+0.200	+0.387	+0.555	+0.696	+0.809	+0.894	+0.954	+0.989	+1.00

$e = .60$

M \ ω	0°	10°	20°	30°	40°	50°	60°	70°	80°	90°
0°	0.000	+0.215	+0.414	+0.585	+0.724	+0.830	+0.908	+0.960	+0.990	+1.00
5	+ .214	.419	.599	.745	.855	.930	.977	.998	.997	[illegible]
10	.406	.593	.748	.864	.942	.985	1.000	.991	.962	[illegible]
15	.566	.730	.856	.941	.987	1.000	.986	.950	.896	[illegible]
20	.692	.831	.929	.984	1.000	.985	.946	.887	.811	[illegible]
30	.863	.952	.995	.995	.961	.900	.820	.726	.621	[illegible]
40	.956	.997	.992	.947	.873	.777	.668	.550	.425	[illegible]
50	.995	.993	.947	.866	.760	.638	.509	.375	.239	[illegible]
60	.997	.958	.877	.765	.634	.494	.350	.207	+ .065	[illegible]
70	.973	.900	.789	.653	.503	.349	.197	+ .049	− .094	[illegible]
80	.923	.826	.690	.534	.370	.207	+ .050	− .099	− .240	[illegible]
90	.868	.740	.584	.412	.239	+ .071	− .088	− .235	− .371	[illegible]
100	.795	.646	.473	.290	+ .110	− .060	− .217	− .360	− .489	[illegible]
110	.713	.546	.359	.168	− .015	− .185	− .337	− .474	− .594	[illegible]
120	.624	.441	.244	+ .048	− .136	− .302	− .448	− .576	− .687	[illegible]
130	.528	.333	.129	− .069	− .251	− .411	− .550	− .668	− .767	[illegible]
140	.427	.223	+ .015	− .182	− .359	− .512	− .641	− .748	− .835	[illegible]
150	.323	.112	− .097	− .291	− .462	− .605	− .723	− .818	− .892	[illegible]
160	.217	+ .002	− .207	− .395	− .557	− .689	− .795	− .876	− .936	[illegible]
170	+ .109	− .108	− .312	− .493	− .644	− .765	− .857	− .924	− .969	[illegible]
180	.000	− .215	− .414	− .585	− .724	− .830	− .908	− .960	− .990	−1.00
190	− .109	− .320	− .511	− .670	− .795	− .886	− .948	− .985	−1.000	[illegible]
200	− .217	− .422	− .602	− .747	− .856	− .931	− .977	− .998	− .997	[illegible]
210	− .323	− .520	− .686	− .816	− .908	− .966	− .995	− .999	− .982	[illegible]
220	− .427	− .612	− .763	− .876	− .949	− .989	−1.000	− .987	− .955	[illegible]
230	− .528	− .698	− .832	− .925	− .979	− .999	− .992	− .963	− .915	[illegible]
240	− .624	− .777	− .891	− .963	− .996	− .997	− .971	− .925	− .861	[illegible]
250	− .713	− .847	− .939	− .989	− .999	− .979	− .935	− .872	− .794	[illegible]
260	− .795	− .907	− .975	−1.000	− .988	− .947	− .884	− .805	− .712	[illegible]
270	− .868	− .954	− .996	− .995	− .959	− .896	− .815	− .720	− .614	[illegible]
280	− .928	− .986	− .999	− .971	− .910	− .827	− .728	− .617	− .499	[illegible]
290	− .973	−1.000	− .982	− .925	− .839	− .735	− .619	− .495	− .366	[illegible]
300	− .997	− .990	− .939	− .852	− .742	− .618	− .486	− .350	− .213	[illegible]
310	− .995	− .950	− .864	− .748	− .613	− .471	− .326	− .182	− .039	[illegible]
320	− .956	− .870	− .748	− .602	− .446	− .288	− .133	+ .016	+ .159	[illegible]
330	− .863	− .734	− .577	− .404	− .230	− .062	+ .096	.243	.379	[illegible]
340	− .692	− .520	− .331	− .139	+ .045	+ .214	.365	.500	.618	[illegible]
345	− .566	− .375	− .173	+ .024	.207	.370	.512	.634	.738	[illegible]
350	− .406	− .200	+ .009	.205	.381	.532	.659	.764	.848	[illegible]
355	− .214	+ .001	.210	.398	.559	.692	.797	.878	.937	[illegible]
360	0.000	+0.215	+0.414	+0.585	+0.724	+0.830	+0.908	+0.960	+0.990	+1.00

TABLE I (*continued*)

$e = .70$

0°	10°	20°	30°	40°	50°	60°	70°	80°	90°
0.000	+0.240	+0.454	+0.629	+0.762	+0.858	+0.925	+0.968	+0.992	+1.000
+ .278	.501	.684	.820	.912	.967	.994	1.000	.988	.960
.502	.695	.840	.934	.984	1.000	.991	.963	.921	.865
.665	.824	.931	.987	1.000	.983	.944	.890	.824	.747
.780	.908	.979	1.000	.982	.937	.876	.801	.718	.625
.920	.987	.998	.962	.895	.810	.714	.611	.504	.393
.983	.998	.959	.880	.777	.663	.544	.425	.305	+ .184
1.000	.970	.890	.777	.647	.512	.380	.250	+ .123	− .002
.986	.918	.803	.663	.513	.365	.222	+ .087	− .041	− .166
.950	.848	.706	.544	.379	.222	+ .075	− .062	− .190	− .311
.899	.767	.601	.423	.248	+ .085	− .063	− .199	− .323	− .439
.834	.678	.493	.302	+ .121	− .044	− .192	− .324	− .443	− .551
.760	.583	.383	.183	− .002	− .166	− .311	− .437	− .549	− .649
.679	.483	.272	+ .066	− .119	− .281	− .420	− .540	− .644	− .734
.592	.381	.161	− .047	− .230	− .387	− .520	− .631	− .726	− .806
.500	.277	+ .052	− .156	− .336	− .486	− .610	− .713	− .797	− .866
.404	.173	− .056	− .261	− .435	− .577	− .692	− .784	− .857	− .915
.305	+ .068	− .161	− .362	− .528	− .660	− .764	− .845	− .907	− .952
.204	− .036	− .262	− .456	− .613	− .735	− .827	− .896	− .946	− .979
+ .102	− .139	− .361	− .546	− .691	− .801	− .881	− .937	− .974	− .995
.000	− .240	− .454	− .629	− .762	− .858	− .925	− .968	− .992	−1.000
− .102	− .338	− .543	− .705	− .824	− .906	− .959	− .988	−1.000	− .995
− .204	− .433	− .627	− .774	− .878	− .945	− .983	− .999	− .997	− .979
− .305	− .524	− .704	− .836	− .923	− .974	− .997	− .998	− .983	− .952
− .404	− .611	− .775	− .889	− .958	− .992	−1.000	− .987	− .958	− .915
− .500	− .693	− .838	− .933	− .983	−1.000	− .991	− .964	− .922	− .866
− .592	− .768	− .893	− .967	− .997	− .996	− .971	− .929	− .874	− .806
− .679	− .835	− .938	− .990	− .999	− .979	− .938	− .881	− .813	− .734
− .760	− .894	− .972	−1.000	− .987	− .948	− .890	− .820	− .739	− .649
− .834	− .942	− .994	− .995	− .961	− .902	− .828	− .743	− .651	− .551
− .899	− .978	−1.000	− .975	− .917	− .838	− .748	− .651	− .548	− .439
− .950	− .997	− .988	− .935	− .853	− .755	− .650	− .540	− .427	− .311
− .986	− .997	− .954	− .871	− .766	− .649	− .529	− .409	− .288	− .166
−1.000	− .971	− .892	− .779	− .649	− .516	− .383	− .253	− .127	− .002
− .983	− .910	− .792	− .649	− .497	− .348	− .205	− .070	+ .059	+ .184
− .920	− .799	− .641	− .468	− .297	− .136	+ .012	+ .149	.275	.393
− .780	− .608	− .411	− .214	− .030	+ .135	.281	.409	.523	.625
− .665	− .466	− .253	− .047	+ .138	.299	.437	.556	.658	.747
− .502	− .280	− .055	+ .153	.333	.484	.608	.711	.795	.865
− .278	− .040	+ .188	.387	.551	.681	.782	.860	.918	.960
0.000	+0.240	+0.454	+0.629	+0.762	+0.858	+0.925	+0.968	+0.992	+1.000

$e = .80$

0°	10°	20°	30°	40°	50°	60°	70°	80°	90°
0.000	+0.282	+0.519	+0.693	+0.813	+0.893	+0.945	+0.977	+0.994	+1.000
+ .385	.630	.808	.917	.975	.997	.998	.984	.958	.923
.624	.819	.939	.991	.999	.979	.943	.897	.843	.782
.769	.918	.989	.997	.967	.917	.856	.789	.717	.640
.862	.970	1.000	.973	.914	.841	.762	.680	.595	.508
.962	1.000	.964	.883	.782	.677	.574	.473	.374	.274
.997	.978	.891	.771	.641	.515	.397	.286	.179	+ .075
.995	.927	.800	.649	.499	.360	.233	+ .117	+ .008	− .098
.969	.859	.699	.526	.361	.214	+ .082	− .036	− .145	− .248
.925	.780	.593	.402	.228	+ .076	− .057	− .175	− .281	− .381
.868	.693	.484	.281	+ .101	− .053	− .185	− .300	− .403	− .497
.801	.600	.375	.163	− .020	− .174	− .303	− .413	− .510	− .598
.727	.504	.266	+ .048	− .135	− .286	− .411	− .515	− .606	− .686
.647	.406	.158	− .062	− .244	− .390	− .508	− .607	− .690	− .762
.562	.307	+ .052	− .168	− .345	− .486	− .597	− .688	− .763	− .827
.474	.206	− .052	− .269	− .441	− .574	− .677	− .759	− .826	− .881
.382	.106	− .152	− .365	− .529	− .653	− .748	− .821	− .879	− .924
.289	+ .007	− .250	− .456	− .611	− .725	− .810	− .874	− .922	− .957
.193	− .091	− .344	− .541	− .686	− .790	− .864	− .917	− .955	− .981
+ .097	− .188	− .434	− .620	− .753	− .846	− .909	− .952	− .980	− .995
0.000	− .282	− .519	− .693	− .813	− .893	− .945	− .977	− .994	−1.000
− .097	− .373	− .599	− .760	− .866	− .932	− .972	− .993	−1.000	− .995
− .193	− .462	− .674	− .819	− .910	− .963	− .990	−1.000	− .996	− .981
− .289	− .547	− .743	− .872	− .947	− .985	− .999	− .997	− .982	− .957
− .382	− .627	− .806	− .916	− .974	− .997	− .998	− .984	− .959	− .924
− .474	− .703	− .862	− .952	− .992	−1.000	− .987	− .961	− .926	− .881
− .562	− .773	− .910	− .979	−1.000	− .991	− .965	− .928	− .881	− .827
− .647	− .836	− .949	− .995	− .997	− .972	− .932	− .883	− .826	− .762
− .727	− .891	− .978	−1.000	− .981	− .940	− .887	− .826	− .759	− .686
− .801	− .938	− .995	− .992	− .953	− .895	− .827	− .755	− .679	− .598
− .868	− .973	−1.000	− .970	− .909	− .834	− .753	− .670	− .585	− .497
− .925	− .995	− .988	− .930	− .848	− .756	− .662	− .569	− .476	− .381
− .969	− .999	− .957	− .870	− .766	− .658	− .552	− .449	− .349	− .248
− .995	− .982	− .902	− .785	− .658	− .535	− .418	− .308	− .202	− .098
− .997	− .936	− .814	− .667	− .519	− .381	− .256	− .140	− .030	+ .075
− .962	− .845	− .680	− .503	− .336	− .187	− .056	+ .063	+ .172	.274
− .862	− .683	− .473	− .269	− .088	+ .066	+ .198	.312	.414	.508
− .769	− .557	− .325	− .110	+ .073	.226	.353	.461	.555	.640
− .624	− .378	− .128	+ .093	.273	.418	.534	.631	.712	.782
− .385	− .109	+ .149	.362	.527	.651	.746	.819	.877	.923
0.000	+0.282	+0.519	+0.693	+0.813	+0.893	+0.945	+0.977	+0.994	+1.000

TABLE I (*continued*)

$e = .90$

$M \backslash \omega$	0°	10°	20°	30°	40°	50°	60°	70°	80°	90°
0°	0.000	+0.375	+0.641	+0.798	+0.887	+0.939	+0.970	+0.988	+0.997	+1.00
5	+ .550	.823	.957	.998	.995	.973	.944	.911	.875	.83
10	.752	.944	1.000	.979	.931	.877	.822	.768	.714	.65
15	.860	.989	.987	.925	.849	.774	.704	.638	.574	.50
20	.925	1.000	.953	.860	.763	.674	.594	.520	.449	.37
30	.987	.975	.859	.721	.595	.487	.394	.311	.233	+ .15
40	1.000	.917	.750	.581	.437	.318	.218	+ .130	+ .050	− .02
50	.983	.842	.636	.444	.289	.164	+ .060	− .029	− .109	− .18
60	.947	.757	.520	.313	.150	+ .022	− .082	− .170	− .249	− .32
70	.897	.666	.405	.188	+ .021	− .107	− .210	− .296	− .372	− .44
80	.837	.571	.292	+ .068	− .100	− .226	− .326	− .409	− .481	− .54
90	.770	.474	.181	− .046	− .212	− .335	− .431	− .510	− .578	− .63
100	.696	.376	+ .074	− .154	− .316	− .435	− .526	− .600	− .663	− .71
110	.618	.278	− .030	− .256	− .413	− .527	− .612	− .680	− .737	− .78
120	.535	.180	− .130	− .351	− .503	− .609	− .688	− .750	− .801	− .84
130	.450	+ .083	− .227	− .441	− .585	− .684	− .756	− .811	− .856	− .89
140	.363	− .013	− .318	− .525	− .659	− .750	− .815	− .863	− .901	− .93
150	.274	− .107	− .406	− .602	− .727	− .809	− .866	− .907	− .938	− .96
160	.183	− .199	− .489	− .674	− .788	− .860	− .909	− .942	− .966	− .98
170	+ .092	− .288	− .568	− .739	− .841	− .904	− .943	− .969	− .986	− .99
180	.000	− .375	− .641	− .798	− .887	− .939	− .970	− .988	− .997	−1.00
190	− .092	− .459	− .709	− .850	− .926	− .967	− .988	− .998	−1.000	− .99
200	− .183	− .539	− .771	− .895	− .957	− .986	− .998	−1.000	− .994	− .98
210	− .274	− .615	− .827	− .933	− .980	− .997	−1.000	− .993	− .980	− .96
220	− .363	− .686	− .876	− .963	− .994	−1.000	− .992	− .977	− .957	− .93
230	− .450	− .752	− .918	− .984	−1.000	− .993	− .976	− .952	− .925	− .89
240	− .535	− .813	− .952	− .997	− .996	− .977	− .950	− .918	− .883	− .84
250	− .618	− .868	− .978	−1.000	− .983	− .951	− .913	− .874	− .832	− .78
260	− .696	− .914	− .994	− .992	− .958	− .913	− .866	− .818	− .769	− .71
270	− .770	− .953	−1.000	− .973	− .921	− .864	− .807	− .751	− .696	− .63
280	− .837	− .981	− .993	− .941	− .871	− .801	− .735	− .672	− .610	− .54
290	− .897	− .997	− .972	− .893	− .806	− .723	− .648	− .577	− .510	− .44
300	− .947	− .998	− .933	− .828	− .723	− .628	− .544	− .467	− .394	− .32
310	− .983	− .980	− .873	− .740	− .617	− .511	− .419	− .337	− .260	− .18
320	−1.000	− .937	− .785	− .624	− .485	− .369	− .270	− .183	− .103	− .02
330	− .987	− .856	− .657	− .469	− .315	− .191	− .088	+ .001	+ .082	+ .15
340	− .925	− .716	− .467	− .255	− .090	+ .038	+ .142	.230	.307	.37
345	− .860	− .607	− .334	− .112	+ .055	.183	.284	.368	.442	.50
350	− .752	− .450	− .155	+ .072	.238	.360	.455	.533	.599	.65
355	− .550	− .196	+ .114	.336	.488	.596	.676	.739	.791	.83
360	0.000	+0.375	+0.641	+0.798	+0.887	+0.939	+0.970	+0.988	+0.997	+1.00

TABLE II. MEAN ANOMALY AT MAXIMUM AND MINIMUM

$e \backslash \omega$	0°	10°	20°	30°	40°	50°	60°	70°	80°	90°
0.10	84.3	74.3	64.5	54.9	45.5	36.2	27.0	18.0	9.0	0.0
	275.7	265.6	255.3	244.8	234.2	223.5	212.7	201.9	190.9	180.0
0.20	78.5	68.5	58.9	49.6	40.7	32.2	23.9	15.8	7.8	0.0
	281.5	271.1	260.4	249.4	238.1	226.7	215.1	203.5	191.9	180.0
0.30	72.8	62.6	53.1	44.1	35.8	27.9	20.6	13.5	6.7	0.0
	287.2	276.4	265.2	253.5	241.6	229.4	217.1	204.8	192.4	180.0
0.40	67.1	56.6	47.0	38.4	30.6	23.6	17.2	11.2	5.5	0.0
	292.9	281.6	269.6	257.2	244.4	231.5	218.6	205.7	192.8	180.0
0.50	61.4	50.4	40.8	32.5	25.3	19.2	13.8	8.9	4.4	0.0
	298.6	286.6	273.6	260.1	246.5	232.8	219.4	206.1	193.0	180.0
0.60	55.6	44.0	34.2	26.3	19.9	14.7	10.4	6.6	3.2	0.0
	304.4	291.1	276.8	262.1	247.4	233.0	219.2	205.8	192.8	180.0
0.70	49.9	37.2	27.3	19.9	14.4	10.3	7.1	4.5	2.2	0.0
	310.1	295.1	278.7	262.2	246.4	231.5	217.7	204.7	192.2	180.0
0.80	44.2	29.6	19.6	13.1	8.9	6.1	4.1	2.5	1.2	0.0
	315.8	297.6	277.9	259.1	242.2	227.3	214.1	202.1	190.9	180.0
0.90	38.4	20.2	10.6	6.0	3.7	2.4	1.5	0.9	0.4	0.0
	321.6	295.8	269.7	248.1	231.2	217.8	206.7	197.1	188.3	180.0

sion of the plot is necessary, that is, rotation in its own plane by 180°, the periastron angle becomes 360° − ω, as given on the standard curves. If the plot is turned over on a horizontal axis, the periastron angle becomes 180° + ω; if turned over on a vertical axis, the angle becomes 180° − ω. Reference may also be made to Figure which compares the light-time curves for $e = 0.$ and $\omega = 0°, 45°, 90°, 135°, 180°, 225°, 270°$ an 315°. In this figure the curves have been shifte horizontally to line up maxima. It should b noted that they do *not* represent the same orbit

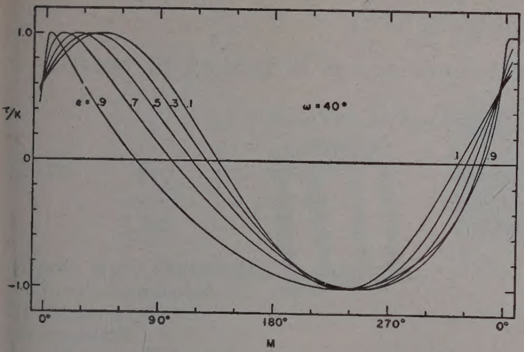

Figure 1. A set of standard light-time curves for five values of the orbital eccentricity. Four additional sets for $\omega = 0°$, 20°, 60° and 80° would give a complete set of such curves.

ellipse as "viewed" from different ω's because of the factor $(1 - e^2 \cos^2 \omega)^{\frac{1}{2}}$ involved in K (see equation 3). For small or moderate eccentricities the shape of a light-time curve closely approximates the shape of a velocity curve having half the eccentricity and with ω decreased by 90°.

Standard velocity curves are used in the analysis of a spectroscopic binary to get good approximate orbital elements preparatory to a least-squares solution by means of differential corrections. The same tactics may occasionally be useful in this problem. Although there are few cases at present where such a least-squares solution would be appropriate, the number of such cases will increase with time. The equations of condition will be of the form:

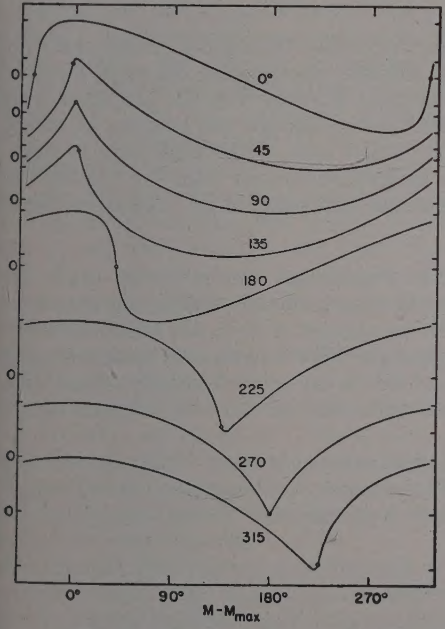

Figure 2. The changing shape of a standard light-time urve for different values of ω is exhibited for $e = 0.9$. he open circles indicate the time of periastron.

$$\Delta\tau_{(o-c)} = b\Delta(a \sin i) + d\Delta\omega + f\Delta e + g\Delta n + h\Delta T + j\Delta t_0 + k\Delta P' \qquad (4)$$

where

$$\begin{aligned}
b &= \frac{\tau}{a \sin i} \\
d &= \frac{a \sin i}{57.3\, c}\left\{\frac{1 - e^2}{1 + e \cos v}\cos(v + \omega) + e \cos \omega\right\} \\
f &= \frac{a \sin i \cos(v + \omega) \sin v}{c(1 + e \cos v)} \\
g &= \frac{a \sin i(t - T)}{57.3\, c\sqrt{1 - e^2}} \times \{\cos(v + \omega) + e \cos \omega\} \\
h &= \frac{-na \sin i}{57.3\, c\sqrt{1 - e^2}} \times \{\cos(v + \omega) + e \cos \omega\} \\
j &= -1 \\
k &= -E
\end{aligned} \qquad (5)$$

With these coefficients the units of $\Delta\tau$, Δt_0 and $\Delta P'$ are days; $\Delta(a \sin i)$ is in kilometers; $\Delta\omega$ is in degrees; Δe is dimensionless; Δn is in degrees/yr ($n = 360°/P$); ΔT is in years. E is not the eccentric anomaly but comes from (1), and c, the velocity of light, is 2.590×10^{10} km/day. Differential coefficients given by Scott (1940) refer to a different reference plane, are in different units, and are given in terms of the eccentric anomaly. Vasilieva (1948) has pointed out an error in Scott's coefficient for Δe, namely: the term $\sin E/(1 - e \sin E)(1 - e^2)^{\frac{1}{2}}$ should be replaced by $\sin E/(1 - e \cos E)(1 - e^2)^{\frac{1}{2}}$. Because of the nature of the problem and especially because of the difficulty in determining the correct value of the period P' of the eclipsing binary, a satisfactorily definitive orbit is difficult of attainment unless at least two successive maxima or minima have been observed.

REFERENCES

Irwin, J. B. 1952, *Ap. J.* **116**, 211.
King, E. S. 1920, *Ann. Harv. Coll. Obs.* **81**, 231.
Schlesinger, F. and Udick, S. 1912, *Pub. Allegheny Obs.* **2**, 155.
Scott, R. M. 1940, *Bull. Harv. Coll. Obs.* No. 912, 3.
Vasilieva, A. A. 1948, *Astr. Circ. Acad. Sci. USSR* No. 75, 12.
Woltjer, J. 1922, *B. A. N.* **1**, 93.

NOTES AND OBSERVATIONS

DETERMINATION OF THE FIRST CONTACT OF THE SOLAR ECLIPSE OF OCTOBER 12, 1958

This eclipse was seen in Chile near sunset, under exceptionally good weather conditions. At our Observatory ($\lambda = 4^{h}42^{m}44\overset{s}{.}4$, $\varphi = -33°33'40''$, $h = 568$ m) the first contact was determined from a sequence of fourteen photographs (diameter of the image = 21 mm) taken by A. Gutiérrez within an interval of $2^{m}25^{s}$ after the contact.

The chords were measured and the reductions made independently by A. Gutiérrez and G. Romero, by means of Danjon's method.

The final results are:

Computer	T_1 (UT)	m.e.	Sets of measure
Gutiérrez	$21^{h}35^{m}20\overset{s}{.}1$	$\pm 0\overset{s}{.}2$	3
Romero	21 35 23.7	±0.7	1

A. Gutiérrez and G. Romer
Astronomical Observator
University of Chi
Santiago, Chi
Received November 25, 195

ADDENDUM

To Symposium on Planetary Radio Astronomy, *Astronomical Journal* **64**, 37–48, 1959: Thi symposium was sponsored by the National Science Foundation. The Committee in charge of th symposium wishes to record an expression of thanks to the National Science Foundation for it support.

NOTICES

Monograph Prizes. The American Academy of Arts and Sciences will award annually three prize of $1000 each to the authors of especially meritorious unpublished monographs, one each in the fiel of the Humanities, Social Sciences and Physical and Biological Sciences. For the purposes of thes awards a Monograph is defined as a "scholarly contribution to knowledge, too long for an article i a learned journal and too specialized or too short for a general book." The final date in 1959 f receipt of manuscripts is October 1. Full details may be secured on request from the Committee o Monograph Prizes, American Academy of Arts and Sciences, 280 Newton St., Brookline Statio Boston 46, Mass.

Kitt Peak National Observatory. Observing with the 36-telescope can probably begin abo January 1960. In reply to several inquiries about observing time received to date, astronomers a informed that requests for use of the facilities, subject to unexpected delays, will be welcomed.

The 36-inch and the 16-inch telescopes will be equipped for UBV photometry with refrigerate photomultipliers. A classification spectrograph will be added to the 36-inch shortly after Janua 1960. A ratio spectrometer is currently available on the 16-inch and a similar unit will soon be adde to the 36-inch.

Observing time can be assigned to a limited number of graduate students for Ph.D. thesis researc Subject to the availability of funds, travel expenses and subsistence will be granted to students.

Applications should be sent to the Director, Kitt Peak National Observatory, 1033 North Pa Ave., Tucson, Arizona.